Estimating the fire growth potential in corridors and tunnels

Jörgen Carlsson

FOI-R-- 1818 --SE
ISSN 1650-1942

Weapons and Protection
Technical report

December 2005

Estimating the fire growth potential in corridors and tunnels

FOI-R--1818--SE
ISSN 1650-1942

Weapons and Protection
Technical report

October 2005

Issuing organization	Report number, ISRN	Report type
FOI – Swedish Defence Research Agency Weapons and Protection SE-147 25 Tumba	FOI-R--1818--SE	Technical report
	Research area code 5. Strike and protection	
	Month year December 2005	**Project no.** E2007
	Sub area code	
	Sub area code 2 51 Weapons and Protection	

Author/s (editor/s)	Project manager
Jörgen Carlsson	Gunnar Wijk
	Approved by
	Sponsoring agency
	Scientifically and technically responsible

Report title

Estimating the fire growth potential in corridors and tunnels

Abstract

An experimental study is presented in which the influence of ventilation on the heat release rate in a long and narrow room, such as a corridor or a tunnel, has been investigated. The experimental rig that was used measured 6.4 metres long and with a cross-section of 1×1 m^2 and a wood-crib was used as fuel source. Radiation is shown to be of major importance and the classical laws of scaling may not be fully applicable.

It is found that there is an almost linear relationship between the ventilation factor and the maximum heat release rate in the enclosure. Furthermore, it is noted that not all of the incoming oxygen is consumed by the fire.

A number of blind simulations using the CFD code FDS were carried out in advance of the actual testing. The stand-alone heat release of the free-burning wooden crib was used as input to the program. The results show good or fair agreement during the initial stages of burning but diverge greatly, producing non-physical results, when the oxygen concentration drops within the enclosure and ventilation becomes a factor. The implication of this being that the combustion models that are currently favoured in fire modelling are inadequate in several scenarios relating to vulnerability studies.

Keywords

Fire, fire growth, fire modelling, underventilated fire, CFD, FDS

Further bibliographic information	Language English
ISSN 1650-1942	**Pages** 52 p.
	Price acc. to pricelist

Utgivare	Rapportnummer, ISRN	Klassificering
FOI - Totalförsvarets forskningsinstitut Vapen och skydd 147 25 Tumba	FOI-R--1818--SE	Teknisk rapport
	Forskningsområde 5. Bekämpning och skydd	
	Månad, år Oktober 2005	**Projektnummer** E2007
	Delområde 51 VVS med styrda vapen	
	Delområde 2	

Författare/redaktör	Projektledare
Jörgen Carlsson	Gunnar Wijk
	Godkänd av
	Uppdragsgivare/kundbeteckning
	Tekniskt och/eller vetenskapligt ansvarig

Rapportens titel

Brandförlopp i avlånga rum, korridorer och tunnlar

Sammanfattning

En experimentell studie har genomförts i syfte att studera ventilationsöppningens inverkan på en brands effekt-utveckling i avlånga geometrier såsom korridorer och tunnlar. Testriggen utgjordes av en 6.4 meter lång inneslutning med ett tvärsnitt av 1×1 m^2 och som brandkälla användes en träribbstapel som i sin tur antändes med 90 ml metanol. Värmestrålningen visade sig vara en avgörande del av värmeflödet och det kan vara svårt att använda de klassiska Froudelagarna för att erhålla en direkt skalning av försöken.

Från testdatan kunde härledas ett nästan linjärt förhållande mellan ventilationsfaktorn och den maximala brandeffekten. I motsats till vad som i teorin kan förväntas visar det sig att inte allt syre förbrukas i branden.

Ett antal a-priori simuleringar genomfördes med CFD programmet FDS innan själva testprogrammet. Som indata används brandeffekten från träribbstapeln uppmätt i fribrinnande miljö. Beräkningsresultaten är bra eller acceptabla i det tidiga skedet av brandförloppet för att i det senare skedet ge helt felaktiga, ofysikaliska, svar. Detta antyder att de förbränningsmodeller som idag används för simulering av brandförlopp har stora begränsningar ur ett verkans-värderingsperspektiv.

Nyckelord

Brand, brandtillväxt, brandmodellering, underventilerad brand, CFD, FDS

Övriga bibliografiska uppgifter	Språk Engelska
ISSN 1650-1942	**Antal sidor:** 52 s.
Distribution enligt missiv	**Pris: Enligt prislista**

Table of contents

Exekutiv sammanfattning (in Swedish)

Följande rapport har tagits fram som en del av projektet Verkansvärdering. Behovet har motiverats av bristen på konsekvent information om hur en underventilerad brand beter sig, framför allt i utrymmen som har ett stort längd/bredd förhållande. Korridorer är ofta en integrerad del i utrymningsstrategin, ibland rent av den enda vägen ut. Samtidigt fungerar korridorer som ledningar för transport av varma och toxiska gaser från en brand. I de fall där andra tilluftsvägar saknas är utförandet på korridoren avgörande för hur en brand utvecklas, detta eftersom den i stor utsträckning styr värmeförluster och lufttillförsel. Detta är många gånger fallet på fartyg. Det finns mycket få brandtekniska utredningar som visar på effekten av längd/bredd förhållandet för brandens intensitet. Det mesta relaterar till tunnelforskning och ger i flera fall motstridiga svar.

Totalt har 14 brandförsök genomförts i en korridor, eller tunnel, av modellskala. Modellen var 6.4 meter lång och hade en tvärsnittsyta av 1×1 m^2. Ett 80-tal mätinstrument registrerade gas- och väggtemperatur, flödeshastigheter, koncentration av syre och brandgaser, värmestrålning och totalt värmeflöde mot vägg och tak med 1 Hz samplingsfrekvens.

Två huvudsyften motiverade genomförandet. Dels söktes ett samband för en brands maximala intensitet och beroendet av ventilation. Dels behövdes experimentella resultat för att kunna utvärdera avancerade brandtekniska beräkningsprogram för dylika scenarier. Militära fordon har mycket små läckytor jämfört med byggnader och arbetar ofta med ett övertryck som skydd mot inträngning av skadliga ämnen. Beräkningarna ger information om hur tillämpbara dagens brandmodeller är för simulering av denna typ av bränder.

Genom att utgå från energi- och massbalansen i ventilationsöppningen och därefter plotta den maximalt uppmätta brandeffekten kunde ett enkelt samband härledas vilket tydligt pekar på kopplingen mellan brandeffekt och ventilationsfaktorn $A\sqrt{H}$ (där A är öppningens area och H är höjden på öppningen). Bilden nedan är densamma som Figure 4 i bulktexten. Sambandet är nästan identiskt med det som brukar användas för att utvärdera övertändning i vanliga rum.

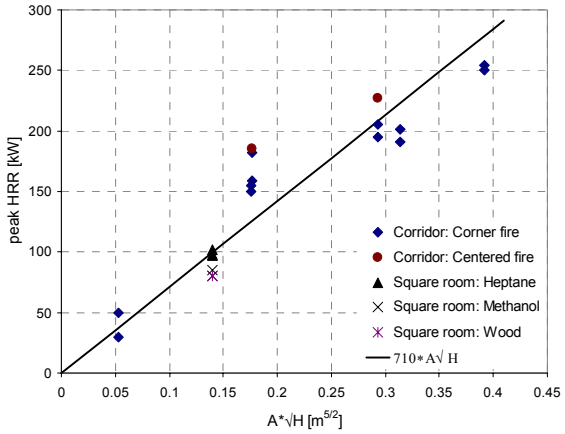

För att utvärdera prediktionsförmågan hos de mest avancerade beräkningsmetoder som används bland praktiserande brandingenjörer idag genomfördes ett antal a-priori, eller ”blinda”, simuleringar innan testseriesns start. Beräkningarna visar på bra prediktiv förmåga i förloppets inledningsskede, då brandeffekten är relativt låg i förhållande till ventilationen. Den använda förbränningsmodellen överskattar dock syreförbrukningen vid brand och ger felaktiga och rent av ofysikaliska resultat när syrehalten i rummet sjunker. I beräkningen leder den sjunkande syrehalten i inneslutningen till att förbränningszonen propagerar över hela korridorens längd och stannar i öppningen där branden fortlöper genom extern förbränning. Klart är att det finns en stor förbättringspotential inom området, behovet av forskning kan inte överskattas.

I det tidiga skedet av brandförloppet ger beräkningarna relativt goda resultat som stämmer överens med observationer och mätdata. Flödeshastigheterna i rummet blir emellertid mycket små, ofta mindre än 0.5 m/s vilket ligger nära eller kanske under gränsen för vad mätutrustningen som använts klarar av att mäta med god precision. Bilden nedan är tagen från Figure 19 och visar kvalitativt på strömningsfältet i korridoren 8 minuter efter brandstart. Röd färg innebär att flödet rör sig utåt mot ventilationsöppningen och blå färg innebär att flödet rör sig innåt. Bilden stämmer överens med observationen att två olika brandgasskikt bildas i korridoren.

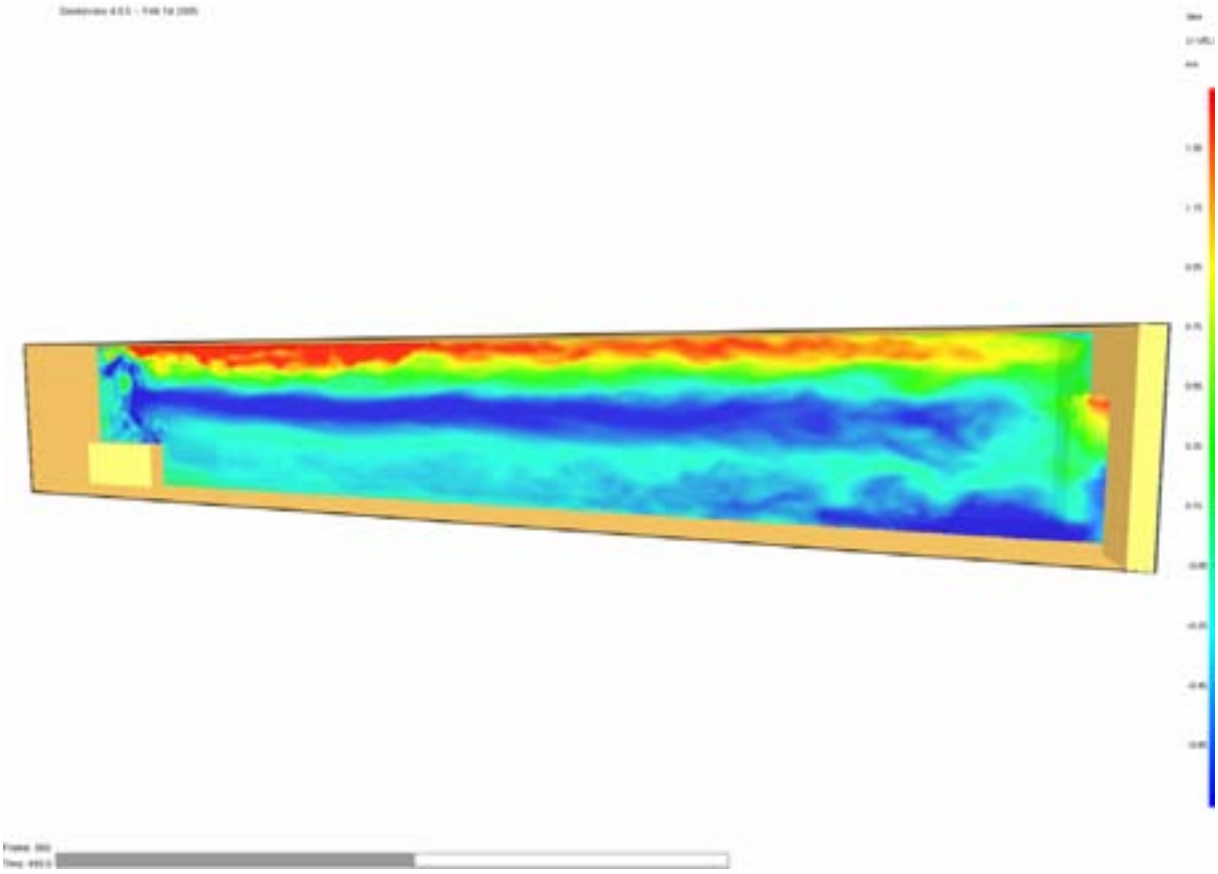

Notation

Below, attention is briefly directed at a number of basic terms and concepts used within the report.

c_p	*specific heat capacity at constant pressure,*
g	*gravity constant (9.8 m/s^2)*
h	*specific enthalpy or heat transfer coefficient,*
k	*thermal conductivity,*
k_a	*gas absorption coefficient,*
k_p	*calibration coefficient of a bi-directional probe, a function of Reynolds number, angle etc,*
k_a	*ratio of the mean duct flow to the flow in the centre of the duct (used in BD-probe equation),*
l	*characteristic length*
m	*mass,*
q	*heat release per unit mass*
t	*time,*
$\mathbf{u}$ *or* U	*velocity vector,*
A	*area of ventilation opening,*
E	*net heat release per unit mass of O_2 consumed (13.1 MJ/kg(O_2) for most hydrocarbon fuels)*
E_{CO}	*net heat release per unit mass of O_2 consumed for combustion of CO to CO_2, 17.6 MJ/kg(O_2)*
H	*height of ventilation opening,*
ΔH_c	*heat of combustion,*
HRR	*Heat Release Rate, dQ/dt,*
I	*radiant intensity,*
I_b	*black body intensity,*
Pr	*Prandtls number,*
Q	*heat release,*
R	*gas constant,*
T	*temperature,*
$X_{O_2}^0$	*measured mole fraction of O_2 in the incoming air (used in the calculation of HRR),*
X_{O_2}	*measured mole fraction of O_2 in the exhaust gases,*
$X_{CO_2}^0$	*measured mole fraction of CO_2 in the incoming air,*
X_{CO_2}	*measured mole fraction of CO_2 in the exhaust gases,*
X_{CO}^0	*measured mole fraction of CO in the incoming air,*
X_{CO}	*measured mole fraction of CO in the exhaust gases,*
$X_{H_2O}^0$	*mole fraction of CO in the incoming air (measured or estimated),*
α	*fuel dependent coefficient in the calculation of HRR (average value of 1.105 are often used),*
δ	*thickness,*
ε	*emissivity,*

Γ	*diffusivity,*
ν	*kinematic viscosity,*
ρ	*density,*
χ	*radiative fraction,*
ϕ	*symbol for an arbitrarily scalar, or oxygen depletion factor (used in the calculation of HRR)*
Ω	*arbitrarily volume in space,*

Superscripts

$''$	*per unit area,*
$'''$	*per unit volume,*
$\dot{}$	*time derivative,*

Subscripts

e	*exhaust*
i, j, k	*unity vectors in the cartesian coordinate system,*
∞	*ambient, or starting, value*

1. Introduction

Corridors often serve as an integral part in the escape strategy of a building or installation in the case of fire. At the same time, the corridors can serve as conduits for transporting hot, toxic combustion gases to other parts of the building making the general characteristics of the fluid flow an essential object of study. Recognising a flashover as being the threshold of survivability for any living being there is a need for studying the limiting scenarios of flashover and under-ventilated fires in corridor-like geometries more in-depth.

1.1 Background

During a number of decades, fires in enclosures - such as the Room Corner test rig and resembling geometries - has been studied extensively resulting in a number of simple hand-calculation tools for estimating gas temperatures, limiting heat release rates and the potential of flashover. Such simplified methods for fire analysis are indeed very useful, not only in assessing survivability of man but also in obtaining an estimate on the thermal insult on load bearing structures and in the end the integrity of the fire compartment and the construction itself.

While the effects of fire in a single, ordinary-shaped, compartment could be predicted to a fair level of accuracy using simple zone-modelling techniques, scenarios involving long, narrow rooms or tall shafts were one major Achilles' heal of early fire modelling. Some efforts were put into the development of add-on algorithms to the computerised zone-model concept although the degrees of success following these attempts were limited.

1.2 Purpose and objective

The purpose of this document is to report on an experimental test series performed using a corridor-shaped construction. The results are discussed from different modelling points of view. Moreover, a simple relationship based on the geometry and ventilation conditions are derived from the experimental data using as a foundation the mass and energy balance. A-priori sample calculations using CFD analysis are carried out to show the modelling capabilities of todays most advanced fire simulation tools in predicting the complex flows and rate of combustion in under-ventilated corridor enclosures.

Although the chosen scenario was studied with a ship interior in mind it is believed that more general lessons can be learnt from the fire modelling exercise of the under-ventilated compartment being the current object of study. Vehicles of war are tightly sealed, usually operating with an over-pressurized compartment, making fire modelling extremely difficult if at all possible using the standard, incompressible, Navier-Stokes equations. The simulations

presented within the present report will give a first hint on the applicability of currently available fire modelling tools.

2. Some related research and background

2.1 General experimental work

While several investigators have reported on tests relating to limiting heat release rates and the potential of flashover in room fires, very few investigations exist in which the room configuration diverge from the standard room. The experiments performed by Factory Mutual[1] for example are useful in evaluating model predictions of smoke movement in a multi-compartment scenario, the details concering heat release rate are, however not available.

Some recent experiments on "corridor" fires are reviewed by Delichatsios and co-workers[2]. They conclude that the burning rate is lower in a corridor-like geometry compared with fires in rectangular, cubic-like, compartments. They study specifically a corridor, open in both ends, and derive, empirically, a relationship for the fuel mass loss rate showing that the maximum burning rate is little more than half of that in an ordinary-shaped enclosure.

On the other hand, Carvel, Jowitt and Drysdale[3] present a comprehensive collection of tunnel data showing higher heat release rates in the tunnel when compared with a free burning case. They argue that the heat release rate of a fire in a tunnel is influenced primarily by the width of the tunnel, suggesting that a fire in a narrow tunnel results in a higher heat release rate compared with a wide tunnel of equal height. Their study was limited to the influence of tunnel geometry on the fire growth but they also advocate that, although not taken into account in their first study, the ventilation conditions in the tunnel may have a far more dramatic influence on the heat release rate than the geometry of the tunnel does.

Reports from several large scale tunnel tests are readily available, one interesting test series being that of Ingason and Lönnermark[4,5]. The objective of the study was to simulate fires involving heavy goods vehicles in a tunnel. In their analysis they use an array of bi-directional probes and gas analyzers in order to estimate the rate of heat release arguing a standard uncertainty of no more than 15 % with a 95 % confidence interval. The tunnel cross-section measured 9×7 m^2 (width×height). Four tests using a mixture of fuels such as wood and plastic pallets, furniture and paper cartons with a total weight between 2850 kg and 11010 kg resulted in a maximum heat release rate of 66-202 MW.

Egan and Litton[6] performed a test series in an intermediate-size tunnel, 10×0.8×0.8 m^3 (length×height×width), using wooden cribs stacked in different shapes. They present a range of measurements including temperature, heat release rate and smoke characteristics (mass concentration, number concentration and average size).

Ingasson, Nireus and Werling[7] carried out a large-scale test series in a blasted rock tunnel. Their tunnel measured 100×3×3 m^3 (length, width, height) ending at a chimney used as an outlet. The rate of heat release was measured in the chimney using a grid of velocity probes and gas analyzers. The position of the fuel, the ventilation conditions and the fuel characteristics were varied. They conclude that, in their tests, the burning rate of liquid fuels shows only a slight dependency to the rate of ventilation while the ventilation influence seems to be more pronounced in the tests using solid fuels.

2.2 Efforts made in computer modelling

In addition to the experimental database a number of attempts have been made to study fires in tunnels and corridors numerically. In the early 1980, Jones and Quintiere[8] compared experimental data on the rate of smoke filling in a corridor connected to a fire room with predictions from different zone-models. Their results show a reasonable agreement with the experiments.

In the late 80's and early 90's the shortcomings of zone-modelling called for the development of submodels capable of more accurately predict smoke movement in corridor geometries. Nelson and Deal[9] implemented an algorithm, based on the equations provided by Steckler[10], called CORRIDOR into the zone-model FPETOOL. The purpose of CORRIDOR was to model the buoyancy driven gravity current of heated gas through a corridor, its forward propagation and the temperature distribution. Several other, even more sophisticated, models were subsequently proposed as submodels to the general zone-model concept.[11,12]

A number of studies using Computational Fluid Dynamics, CFD, have been presented during the last decade and a half. Among the first being Satoh and Miyazaki[13] who simulated tunnel flows. Despite the use of rather sizeable computational grid-nodes they were able to show some interesting features of the flow and a reasonable agreement with experimental data.

Tuovinen[14] simulated ceiling flows in a large corridor, completely open in both ends and with different ceiling vents, using the RANS code JASMINE. The simulations showed predictions within 30% of the measurements. He concludes that there is a need of more well-defined experiments for model comparisons.

2.3 Useful correlations

A number of correlations has been proposed describing a flashover or post-flashover (ventilation-controlled) fire in normal cubic-like enclosures, some of which will be repeated here.

One of the most widespread equations, useful in estimating the room flashover potential, is the correlation derived by McCaffrey, Quintiere and Harkleroad[15]. They derived two

dimensionless groups, one based on the heat release and another based on heat losses through the surrounding walls, and used a substantial collection of experimental data to obtain numbers to their coefficients. The result is a correlation for estimating the gas temperature in a ventilated enclosure.

$$\frac{\Delta T_g}{T_\infty} = 1.6(X_1)^{2/3}(X_2)^{-1/3}$$

where

$$(X_1) = \frac{\dot{Q}}{c_p \rho_\infty T_\infty A_w \sqrt{gH}}$$

$$(X_2) = \frac{h_{eff} A_T}{c_p \rho_\infty T_\infty A_w \sqrt{gH}}$$

If it can be assumed that the thermal wave has reached the unexposed side of the walls and reached a steady state, the effective heat transfer coefficient can be evaluated from:

$$h_{eff} = \frac{k}{\delta}$$

Here k is the thermal conductivity and δ represents the thickness of the wall. However, if a steady state has not been reached, a more appropriate calculation procedure would be that of the equation below, including the thermal inertia of the wall material and the exposure time, t.

$$h_{eff} = \frac{k\rho c_p}{t}$$

Writing the mass balance in an enclosure opening gives an equation for the inflow of air through the vent:

$$\dot{m}_{air} = \frac{2}{3} C_d A \sqrt{H} \rho_\infty \sqrt{2g \frac{(\rho_\infty - \rho_g)}{\rho_\infty \left(1 + \left(\frac{\rho_\infty}{\rho_g}\right)^{1/3}\right)^3}}$$

It is shown in Figure 1 that if the gas temperature is at, or above, 500 °C the expression $\sqrt{\frac{(\rho_\infty - \rho_g)}{\rho_\infty \left(1 + \left(\frac{\rho_\infty}{\rho_g}\right)^{1/3}\right)^3}}$ becomes more or less constant = 0.214.

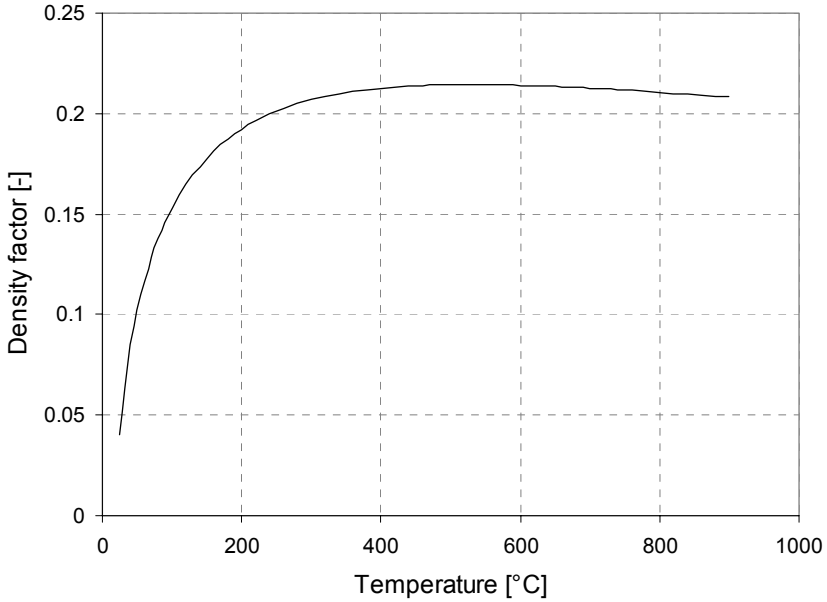

Figure 1 Variation of the density factor with temperature.

Thus, the mass balance can be approximated using $\dot{m}_a \approx 0.5A\sqrt{H}$ where a flow coefficient C_d = 0.7 has been assumed. The maximum rate of heat release that can be sustained in the enclosure can be estimated by replacing the rate of air flow with the oxygen flow rate through the mass fraction of oxygen in air, 0.23, and assuming the general oxygen consumption energy release 13.1 MJ/kg, ending up with:

$$\dot{Q}_{\max} = \dot{m}_{air} Y_{O_2} \Delta H_{c,O_2} \approx 1.5A\sqrt{H} \text{ MW}$$

This gives the maximum, theoretical, rate of heat release. A similar equation can be derived using a simple energy balance in the enclosure opening:

$$\dot{Q} = \dot{m}_{air} c_p dT + \dot{Q}_{losses}$$

Here the first term on the right hand side is the energy contained in the outflowing gases (which by continuity equals the mass flow of inflowing air). $\dot{Q}_{losses}$ represents heat losses through the walls and the ceiling of the enclosure, generally, this term is tricky to estimate.
In comparing results from a sizeable compilation of experiments, Babrauskas[16] concluded that the effective maximum heat release rate was only half of that predicted from the theoretical maximum estimation:

$$\dot{Q}_{effective} = \frac{1}{2} \cdot 1.5A\sqrt{H} = 0.75A\sqrt{H} \text{ MW}$$

In the scenario considered in this work that is, a corridor-like geometry there are some factors to speak against the validity of this relationship. Some of these are:

1) The temperature in the opening is likely to be well below 500 °C although a gas temperature above 200 °C would suffice accepting an error of a few percent.
2) The surface area of the enclosure walls are large compared with the area of the opening which may allow more heat losses.
3) Depending on the position of the fire, the flow of oxygen from the opening may need to move a long distance to reach the combustion zone, thus there may be a diluting effect of the incoming air. Moreover, the inflowing air is likely to lose some of its momentum from the interaction with the upper gas layer in a way that is not encountered in more cubic-like enclosures.

The following report will analyse the fire growth potential in some depth.

3. Experimental method

A number of tests have been carried out using a wood-crib fire in a long and narrow room. The main purposes have been to investigate the characteristics of the flow and to study the applicability of simple correlations for heat release estimations of ventilation-controlled burning in the corridor-like geometry. Moreover, the collected data are quite useful for a variety of computer modelling excersises.

3.1 Fire tests in an intermediate-scale corridor

The model-scale corridor has a cross-section of 1×1 m^2 and measures 6.4 metres in length. The material of the walls, floor and ceiling are either made of 50 mm concrete (2 metres at the lower end of the corridor) or 20 mm Promatec fibre silica board. The concrete was used in order to avoid the massive thermal impact, towards the more fragile Promatec board, that follow from the fire.

The fire consisted of $600\times15\times15$ mm^3 spruce sticks stacked together with 15 mm space to form a $600\times600\times225$ mm^3 (W×D×H) wooden crib. The sticks were stored within a controlled environment until use effectively making the moisture content constant around 9.5 % by mass. The wooden crib was ignited using 0.09 liters of methanol distributed over the crib using three plastic cushions that were ignited using a canthal wire.

A total of 14 tests were carried out, 12 of which had the fire source located in the back corner of the corridor, on the opposite side of the ventilation opening. Among those 12 tests only the size of the ventilation opening were varied. Two tests were made in which the fire were moved forward 1.7 metres and placed on the centreline of the corridor.

Table 1. Summary of tests

Test number	**Ventilation opening B×H [metres]**	**Location of fire**
1,2	0.50×0.85	Back corner
3,6	0.50×0.50	Back corner
4,5	0.15×0.50	Back corner
7,8	0.40×0.85	Back corner
9,10	0.30×0.70	Back corner
11,12	0.50×0.70	Back corner
13	0.50×0.70	Centreline, 1.7 m from the back wall
14	0.50×0.50	Centreline, 1.7 m from the back wall

Figure 2 is a schematic of the test rig including the locations of the different measurement probes. The length of the corridor is divided into slices, 0.50 metres in length starting at the vent. The faces are named A-N, in addition D+ is located 0.25 metres from D and K+ 0.35 v from K as shown in Figure 2. The measurements and the measurement techniques that have been used are briefely described in the following paragraphs.

Temperature: Gas temperatures and wall temperatures were measured using type K chromel-alumel thermocouples, 0.25 mm in diameter.

The temperature distribution in the vent was measured using a vertical thermocouple tree in the centre of the opening.

Four thermpcouple trees were placed at the locations labelled as D and H in Figure 2, both in the centreling and 0.15 metres from the side wall.

In addition, the temperature distribution was measured in the centreline 0.1 metres below the ceiling in the whole length of the corridor with 0.5 metres spacing.

Gas temperatures were further measured at the three BD probes at D+, centrally and at 0.15 metres from both side walls, 0.1 metres below the ceiling.

The temperatures inside the concrete wall were measured at the same location as the wall heat flux gauge. The inner and outer surface temperature of the Promatec board was measured in the centre of the wall and ceiling at the position labelled G in Figure 2.

Gas velocity: The velocities at different locations in the gas flow were evaluated using bi-directional (BD) probes to measure the pressure difference, which can be related to the velocity through the gas density (or temperature) using the relationship:

$$u = \frac{k_t}{k_p(\mathrm{Re})}\sqrt{\frac{2\Delta PT}{\rho_\infty T_\infty}}$$

Gas velocities are measured in two vertical arrays, the one in the opening, at A, and the other on the centreline 3.5 metres from the opening, at H,. Moreover, three bi-directional probes were installed at D+, 1.75 metres from

the opening and 0.1 meter below the ceiling, centrally and at 0.15 metres from the side walls.

Heat flux: The total heat flux to the inner structure was measured at two positions using Schmidt-Boelter type gauges. The water-cooled gauges were placed 1.0 metres from the back wall, at K+, one in the ceiling centreline and another in the centre of the wall.

Radiation: Radiation heat fluxes were measured using water-cooled radiation flux meters of Gunners type. These were positioned at the same locations as were the total heat flux gauges with the addition of one Gunners meter placed in the floor centreline thus facing the ceiling gauge. The position is labelled K+ in Figure 2.

Mass loss: The wooden-crib was placed on top of a weightning floor with load cells located below the floor of the model in order to estimate the initial burning rate. The accuracy of this weighting floor is given to ±1.0 g.

HRR: The rate of heat release was measured by collecting the combustion gases into a duct and within the duct measuring the fluid mass flow rate, and the mole fractions of oxygen, carbon monoxide and carbon dioxide. The relationship for estimating the fire growth can be written[17]

$$\dot{Q} = \left[E\phi - \left(E_{CO} - E\right)\frac{1-\phi}{2}\frac{X_{CO}}{X_{O_2}} \right] \frac{\dot{m}_e}{1+\phi\left(\alpha - 1\right)} \frac{M_{O_2}}{M_a}\left(1 - X^0_{H_2O}\right)X^0_{O_2}$$

where ϕ is the oxygen depletion factor defined as the fraction of the air flowing into the duct that is completely depleted of its oxygen.

$$\phi = \frac{X^0_{O_2}\left(1 - X_{CO_2} - X_{CO}\right) - X_{O_2}\left(1 - X^0_{CO_2}\right)}{\left(1 - X_{O_2} - X_{CO_2} - X_{CO}\right)X^0_{O_2}}$$

Gas analysis: The combustion gases were sampled using an M&C Sampling System PSS. The oxygen concentration was evaluated using an Analyser PMA (0-30 % by volume). Carbon monoxide concentration was measured using a Maihak Finor (0-10 vol%) and a Maihak Unor 6N (0-1000 ppm or 0-10000 ppm) and the concentration of carbon dioxide was measured using a Maihak Finor (0-20 % by volume).

Gas concentration measurements were mainly used for the evaluation of fire heat release rate but were also measured within the corridor 5.0 metres from the vent at K, o the centreline 0.1 metres below the ceiling.

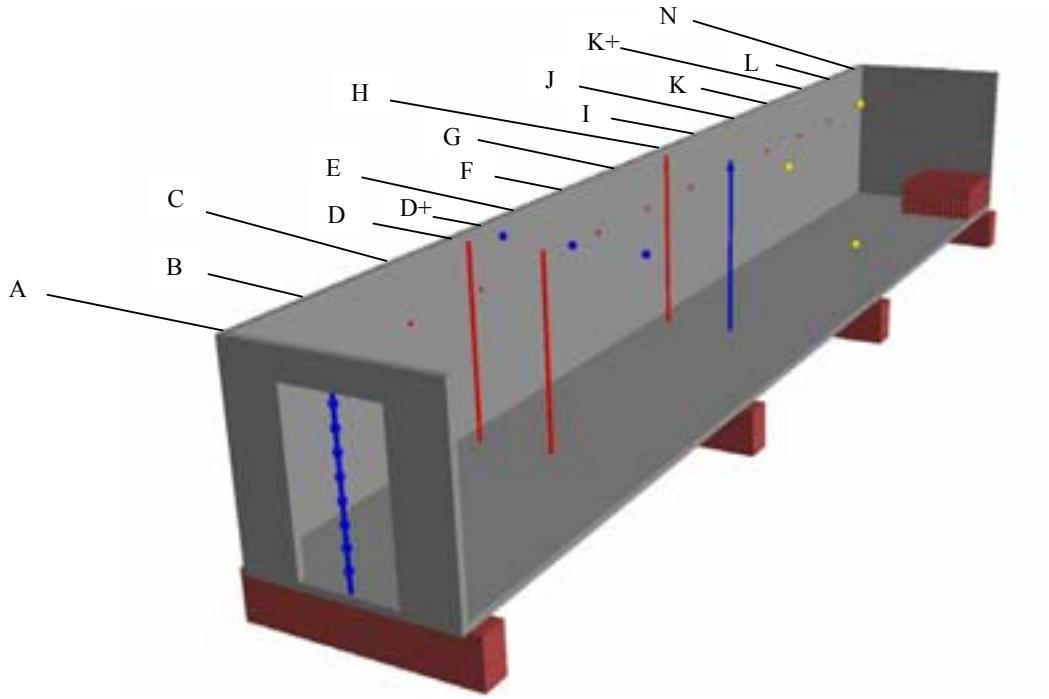

Figure 2. A schematic view of the test rig used in the experiments. Two additional tests were performed in which the wooden crib was moved forward by 1.7 metres and centred in the corridor cross section. Red color indicate thermocouples, blue denote BD-probes and yellow show the position of the heat flux gauges.

3.2 A note on scaling of fires in enclosures

Considering elementary aspects such as performance cost and operational ease, the key benefits from using reduced-scale models, such as the test rig described above, becomes evident. The art of scaling relates to the question of how to obtain results that are representative to the full-scale scenario and optimizing the degree of control in the scaling exercise. The key issue is concerned with the number of dimensionless groups, generally referred to as π-groups, that are conserved from the full-scale fire to the model. The fewer the number of groups the lesser the degree of control.[18] The complexity of chemically reacting flows and constraints imposed by material properties makes it practically impossible to satisfy but a few of the potentially significant dimensionless groups.

The most commonly used technique for correlating enclosure fires of different scales is known as Froude modelling. The basis of Froude modelling are derived from geometric similarity and from the assumption that viscosity effects on the fluid flow are negligible as compared with the effects exerted by inertia and buoyancy forces, thus effectively ignoring the influence of solid boundaries. The π-groups are derived from the dimensionless

conservation equations for mass, momentum, energy and species and their boundary conditions, some of the most essential groups are reproduced here.

i. $\pi_1 = \frac{gl}{u^2} = \frac{1}{\mathrm{Fr}^2}$ which is a measure of the relative importance of inertia and buoyancy effects.

From experimental studies[19] it can be shown that the Froude number, $\mathrm{Fr} = \frac{u}{\sqrt{gl}}$ can be rewritten using the proportionality $\sqrt{\mathrm{Fr}} \propto \frac{\dot{Q}}{l^{5/2}}$, and thus we can write an alternative π_1 as

$\pi_1' = \left(\frac{\dot{Q}}{\rho_\infty c_p T_\infty g^{1/2} l^{5/2}} \right)^{-1} = \frac{1}{\dot{Q}^*}$ where $\dot{Q}^*$ is a non-dimensional heat release rate described using the square root of the Froude number.

ii. $\pi_2 = \frac{\delta^2}{\alpha \tau}$ relating to the thermal wave in solid materials such as walls, floor and ceiling, τ is a reference time (burnout time).

iii. The boundary condition at the solid surface can be written $-k_s \frac{\partial T_s}{\partial x_s} = h(T - T_s) + \dot{q}''_{rad}$. The convective effect is described through the convective heat transfer coefficient $h = \frac{k_{fluid}\mathrm{Nu}}{l}$ where Nu is the Nusselts number which depends on several parameters such as location in the flow field, temperature, geometry and fluid properties. Assuming turbulent flow over a flat plate the average Nusselts number can be written $\mathrm{Nu} = 0.037\mathrm{Re}^{4/5}\mathrm{Pr}^{1/3}$. The Prandtl number depends on the fluid exclusively and thus, for a given fluid at a given temperature, the solid boundary condition gives $\pi_3 = \mathrm{Pr}^{1/3} \frac{k_{fluid} \rho_\infty^{4/5} l^{1/5} \delta}{k_s \mu^{4/5}}$ which measures the relative importance of heat flux by convection to solid conductive heat transfer at the boundary.

iv. Furthermore, from the solid boundary condition we have the effects of radiative heating of hot gases, flames or nearby walls. From this equation we have essentially

two different dimensionless groups, the most important being $\pi_4 = \frac{\varepsilon_s \sigma T_\infty^3 \delta}{k_s}$ which measures the importance of radiation to solid phase conduction.

Moreover, from the radiation equation it follows that the absorptivity of the gas layer should be conserved. It is however, rather impossible to obtain perfect similarity for the gas phase radiative properties which is why $\pi_5 = 1 - e^{-k_a l_{mb}}$ in most cases must be ignored.

Unless the surface emissivity can be adequately manipulated, the groups π_3 and π_4 cannot be satisfied simultaneously. Thus, one of the two is selected based upon the dominating mode of heat transfer, if thermal radiation is expected to be significant π_4 is chosen while π_3 is chosen if convection is expected to be dominating the heat transfer to the walls and interior solids.[20]

Williams[21] derived 28 dimensionless groups needed for complete scaling of fire phenomena and Quintiere[20] shows 14 groups, all of which, ideally, should be conserved in order to obtain similarity between different model scales. Certainly, all of these groups are not as influential as the other and thus, although we only consider a handful of π-groups in the discussion above, this selection is assumed to provide reasonable results. Accordingly, for the same point in time and at corresponding coordinates, the relevant dependent variables will scale as follows:

Rate of Heat Release: $\dot{Q}_M = \left(\frac{l_M}{l_{FS}} \right)^{5/2} \dot{Q}_{FS}$

Flow Velocity: $v_M = \left(\frac{l_M}{l_{FS}} \right)^{1/2} v_{FS}$

Temperature: $T_M = T_{FS}$

Heat flux $q''_M \approx q''_{FS}$

Another scaling technique that has been put to test is known as pressure modelling. In general, the Froude scaling laws are applied but the testing is performed at elevated pressure. de Ris, Kanury and Yuen[22] used this technique successfully adding the extra requirement of preserving the product $\pi_{pressure} = p^2 l^3$.

Scaling according to the technique referred to as analog modelling includes the use of different density fluids in order to simulate fire induced flow, one key example being the salt-water simulation of fire induced gravity currents.

4. Results

Below the main results will be presented and discussed in brief, the main objective of this chapter being to give an overview of the results and their interpretation. The complete set of experimental data is presented in FOI MEMO 1530[24].

With the exception of tests 13 and 14, carried out to obtain a general opinion on the importance of fire location, two tests were performed for each vent configuration. From this it could be concluded that the repeatability of the tests were high except for the cases including the smallest ventilation opening. The discrepancy that can be seen is believed to be connected to the fire initiation using plastic cushions (small bags) of methanol. In case the plastic bag does not rupture instantaneously, the methanol will not be distributed on the wooden sticks but rather cook off inside the bag causing the wooden crib to ignite inhomogenously. This problem is, of course, present in all the tests but since the main objective here is not to evaluate the details of fire growth but rather to obtain information on the ventilation effects on the maximum heat release rate of a corridor fire, this is not considered a big issue.

4.1 Burning rate

Fires are generally characterised by their energy release rate, defined as the mass loss of a fuel times its net heat of combustion. In this test series, a wooden crib measuring 0.6×0.6 m^2 and with a height of 0.225 metres was used. Figure 3 is a diagram of the wood-crib fire in an unconfined mode. It is shown that the effective heat of combustion increases as the rate of smouldering combustion of charcoal increases, after about 30 minutes of burning, flaming combustion is but faint and the measured heat release originates from the glowing of the remaining char.

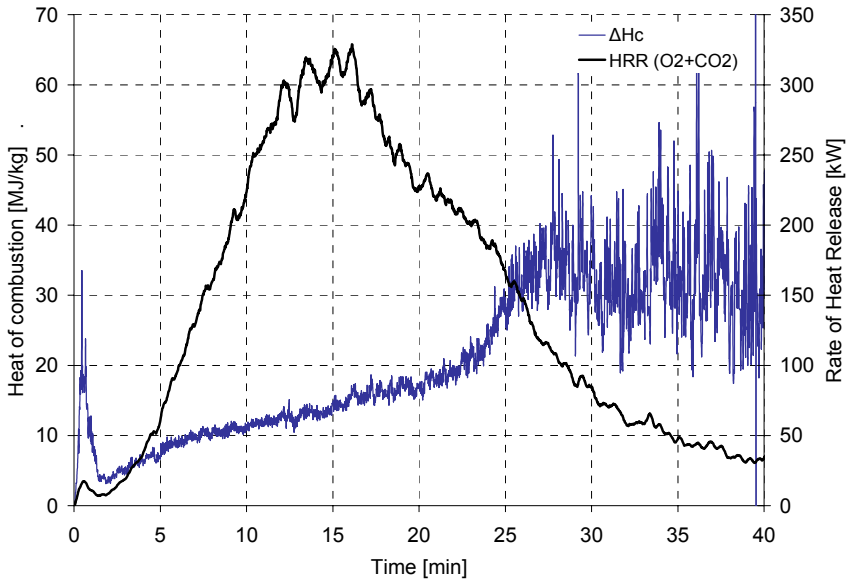

Figure 3. Fire heat release rate and effective heat of combustion for the free burning wooden crib used as fire source in the experiments. The peak HRR is 328 kW.

In the earlier, general, review of enclosure fires it was argued that the rate of heat release is governed primarily by the inflow of oxidant from the enclosure opening and by the heat losses to the surrounding walls. Moreover, it can be argued that the rate of burning is influenced by the location of the fire for example; if the fire is located in a corner two sides are effectively blocked from air entrainment while at the samt time re-radiation from the (subsequently) heated walls also proves to be a factor.

It is clear that one cannot speak in terms of flashover in the examined scenarios. Nevertheless, all of the fires are ventilation controlled rather than being governed by the available amount of fuel. From Figure 4 it is clear that there is a more or less direct proportionality between the ventilation factor, $A\sqrt{H}$, and the maximum rate of heat release within the corridor. The proportionality coefficient, 710, is very close indeed to the one derived by Babrauskas[16] (that is 750). In Figure 4, the results from earlier small-scale testing at FOI[23] have been added for comparison.

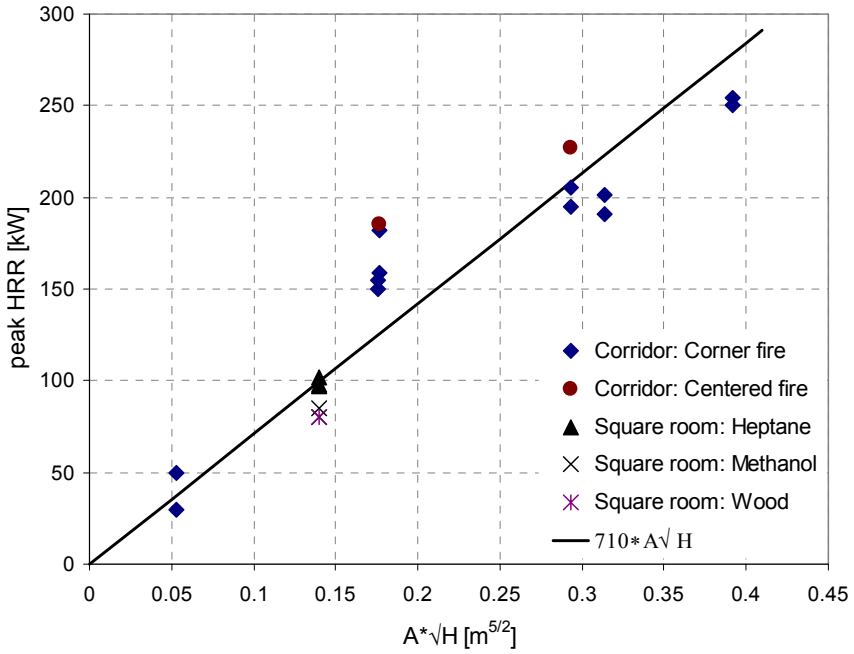

Figure 4. Maximum heat release rate plotted as a function of the ventilation factor. The data labelled “Square room” are taken from reference 23.

Heat losses due to conduction through walls can be roughly estimated using the temperature readings from the embedded thermocouples within the walls and the ceiling. In Figure 5, the heat loss has been estimated assuming steady state heat conduction through the Promatec board and that the data sampled from position G is representative as mean wall temperature. These are not solid assumptions although the calculation should get a general idea of the magnitude of the heat loss term. It appears that the absolute value of the energy loss is rather constant between 15-20 kW except for the tests using a very small ventilation opening. Thus,

the relative heat losses due to heat transfer through the surrounding walls are approximately 10% of the total rate of heat release.

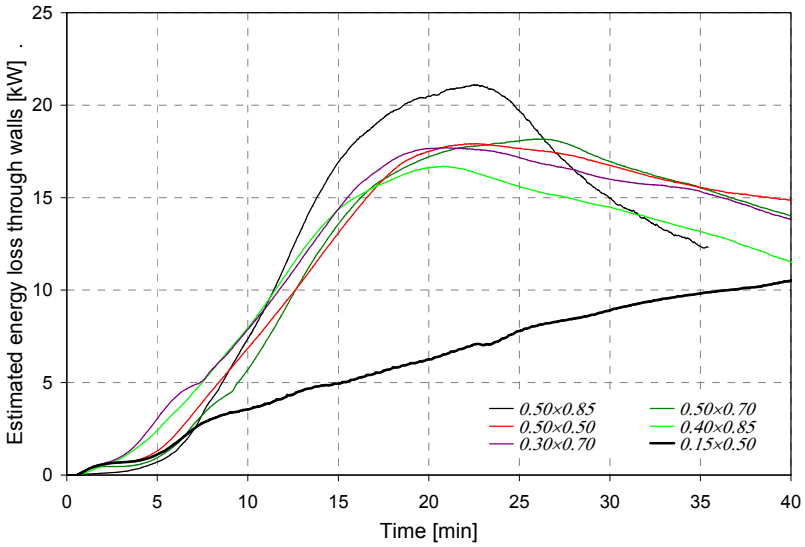

Figure 5. Estimation of the energy lost due to conduction through the surrounding walls. The labels refer to the size of the ventilation opening in metres.

The peak mass loss rate seems to be much more independent of the ventilation factor than does the effective heat release rate. In Figure 6, below, only the one test with the smallest vent size diverges significantly. The trend is thought to be related to the mode of ignition using 90 ml of methanol evenly distributed over the wooden crib, effectively causing the whole crib to pyrolyse. If, however, the methanol bags fail to distribute the fluid in some part of the crib, the lack of thermal insult to that area will cause a delay in the flashover of the crib and may, given the low ventilation rate, cause the large difference in peak mass loss that distinguish the smallest vent in Figure 6.

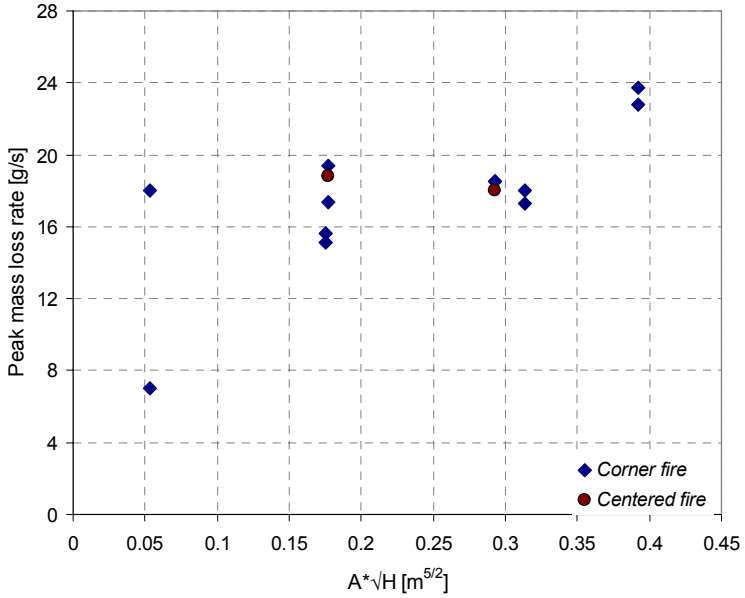

Figure 6. Peak mass loss rate of fuel.

4.2 Gas temperatures

It is intuitively obvious that the gas temperature will vary significantly along the length of the corridor. The maximum ratio of the gas temperature, in degrees Kelvin, at position N (see Figure 2), which is more or less enveloped by the flames in most tests, to the temperature at position B, 0.5 metres from the vent, are about a factor of 2 for all tests. Figure 7 exemplifies the temperature distribution as measured for different ventilation conditions. In Figure 7 f), the steady pulsations (approximately 1 pulsation per 30 seconds) from the massively underventilated fire are distinct.

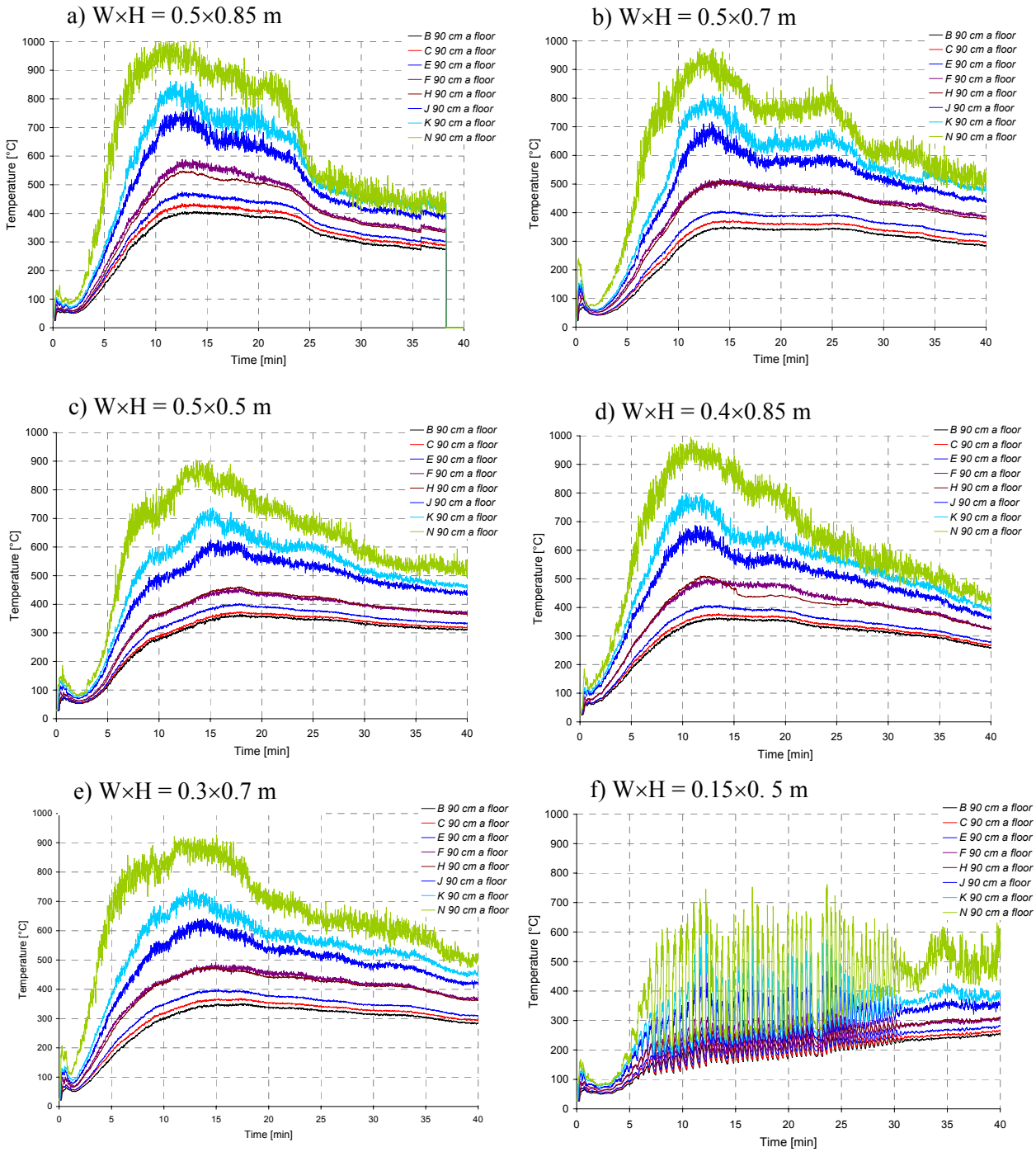

Figure 7. Gas temperature distribution in the centreline 0.9 metres above the floor (0.1 metres below the ceiling).

Figure 8 shows the temperature variation in the centreline of the opening. The position of the neutral layer is located at about half the height of the opening throughout the tests. The temperatures are seldom above 350 °C, which is not sufficient to ignite most practical building materials.

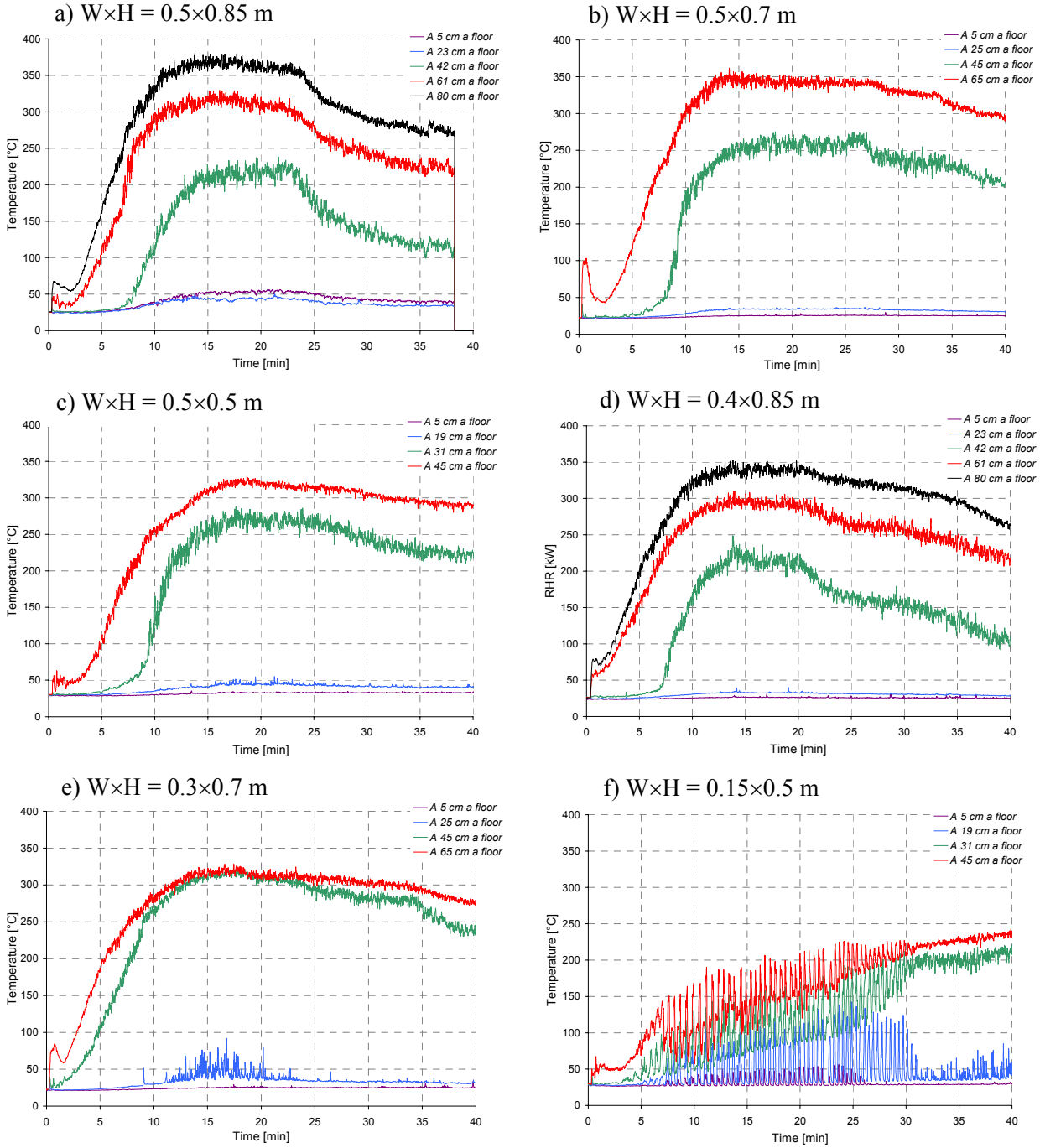

Figure 8. Temperature distribution in the vent centreline. The W×H (Width×Height) product gives the vent dimensions in metres.

From Figure 9 it is clear that the temperature in the cross-section of the uppermost gas layer is rather homogenous.

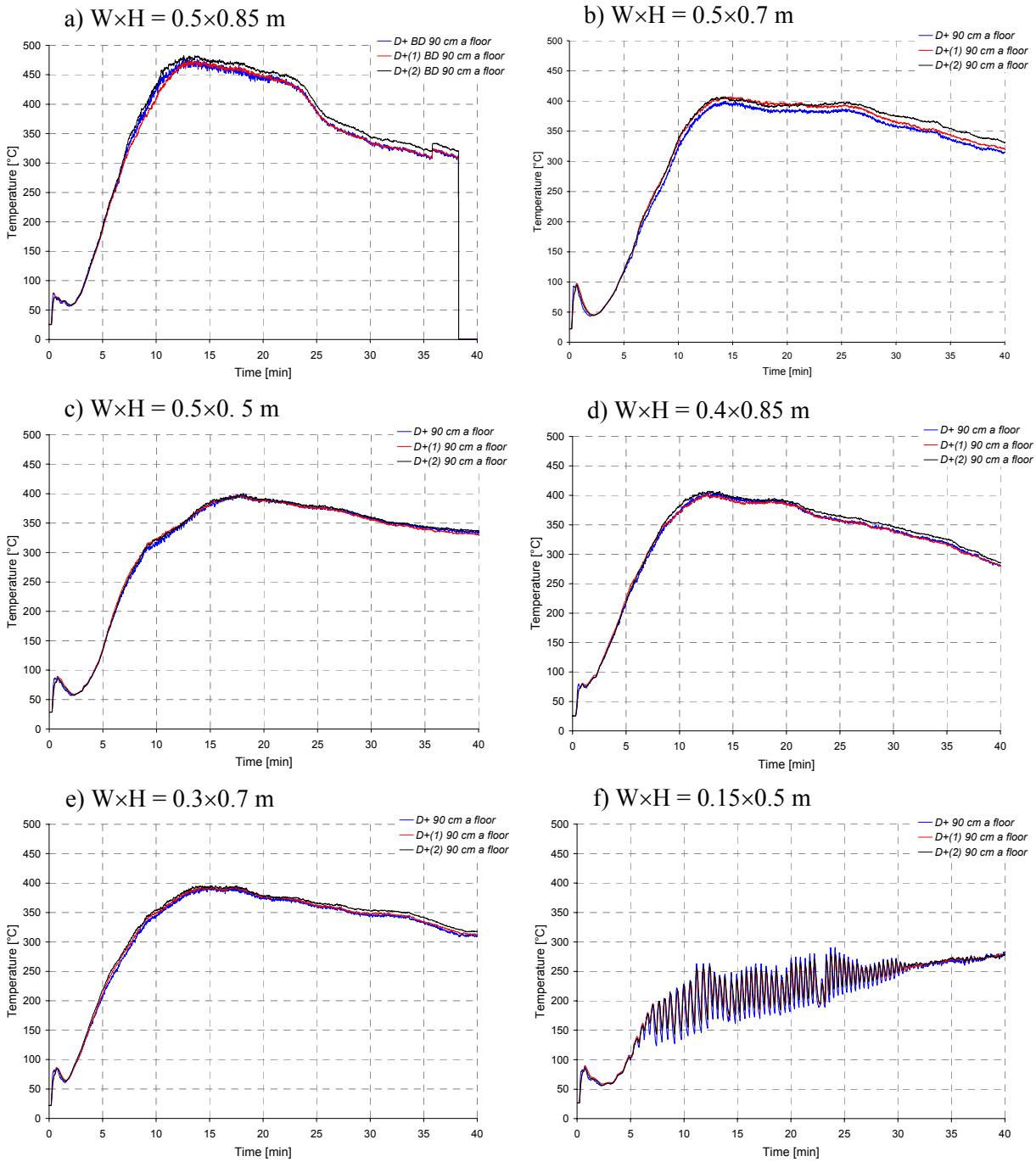

Figure 9. Gas temperatures in the cross section of the corridor 1.75 metres from the opening and 0.1 metres below the ceiling. D+(1) and D+(2) are located 0.15 metres from the side alls.

4.2 Gas velocity

The velocity of the combuston gases were measured in the vertical centreline of the opening, in the cross-section 90 cm above the floor at position D+ and in the centre vertical array at position H, see Figure 2. Combining the velocity measurements in the vent with the temperature the mass balance can be obtained.

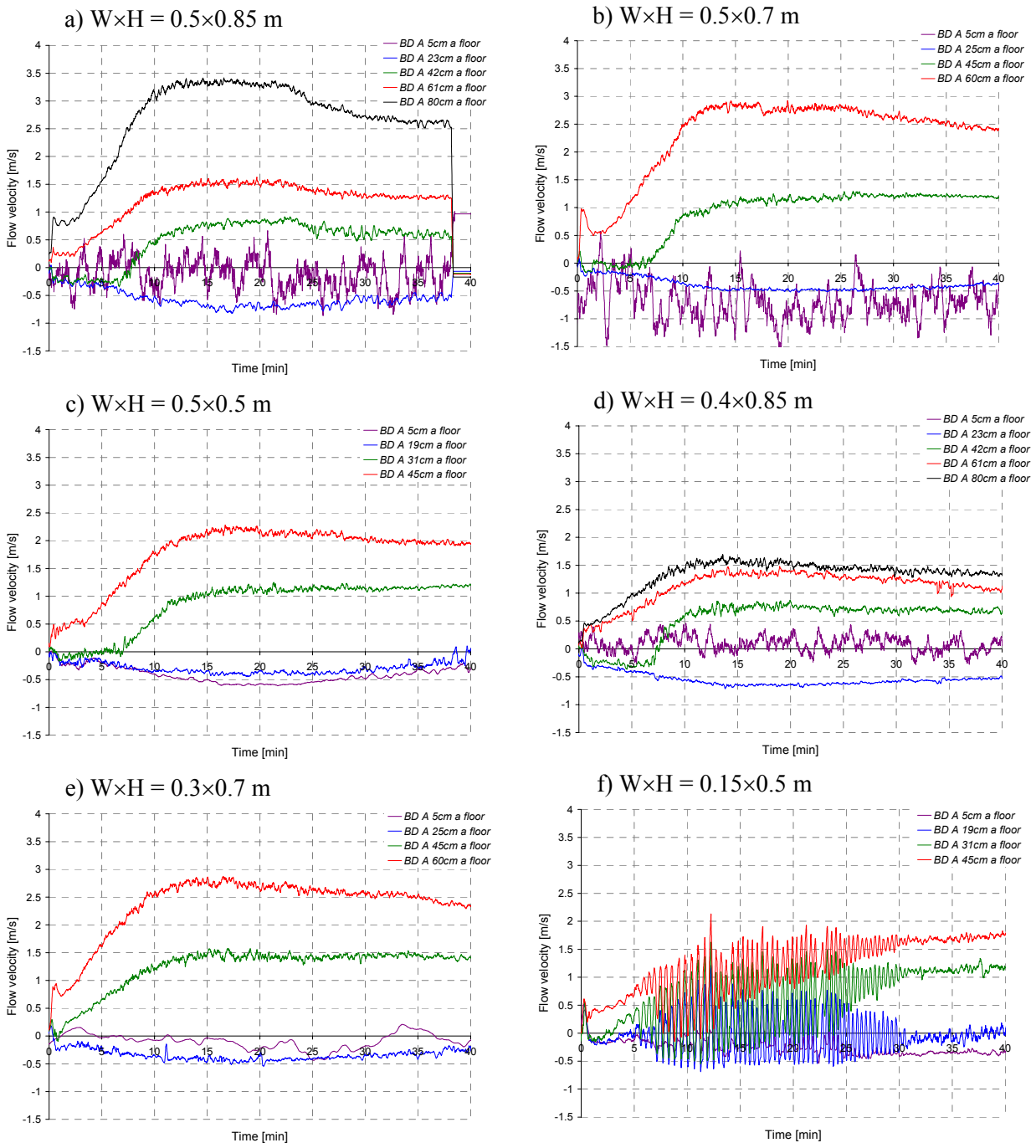

Figure 10. Flow velocity in the ventilation opening.

The flow is very weak, at the very limit of what the pressure transducers can measure correctly. A very interesting feature of the flow in the corridor is revealed in Figure 11. Rather than indicating two gas layers, one hot ceiling jet of combustion gases moving towards the opening and one cold stream of fresh air moving inwards towards the fire, it seems as if several layers of flow exist. Qualitatively, the trend is seen in all scenarios and except for the scenario with the largest opening, Figure 11 a), also the quantitative data are consistent. Furthermore, this is also consistent with the observations of two gas layer interfaces that were made during the tests.

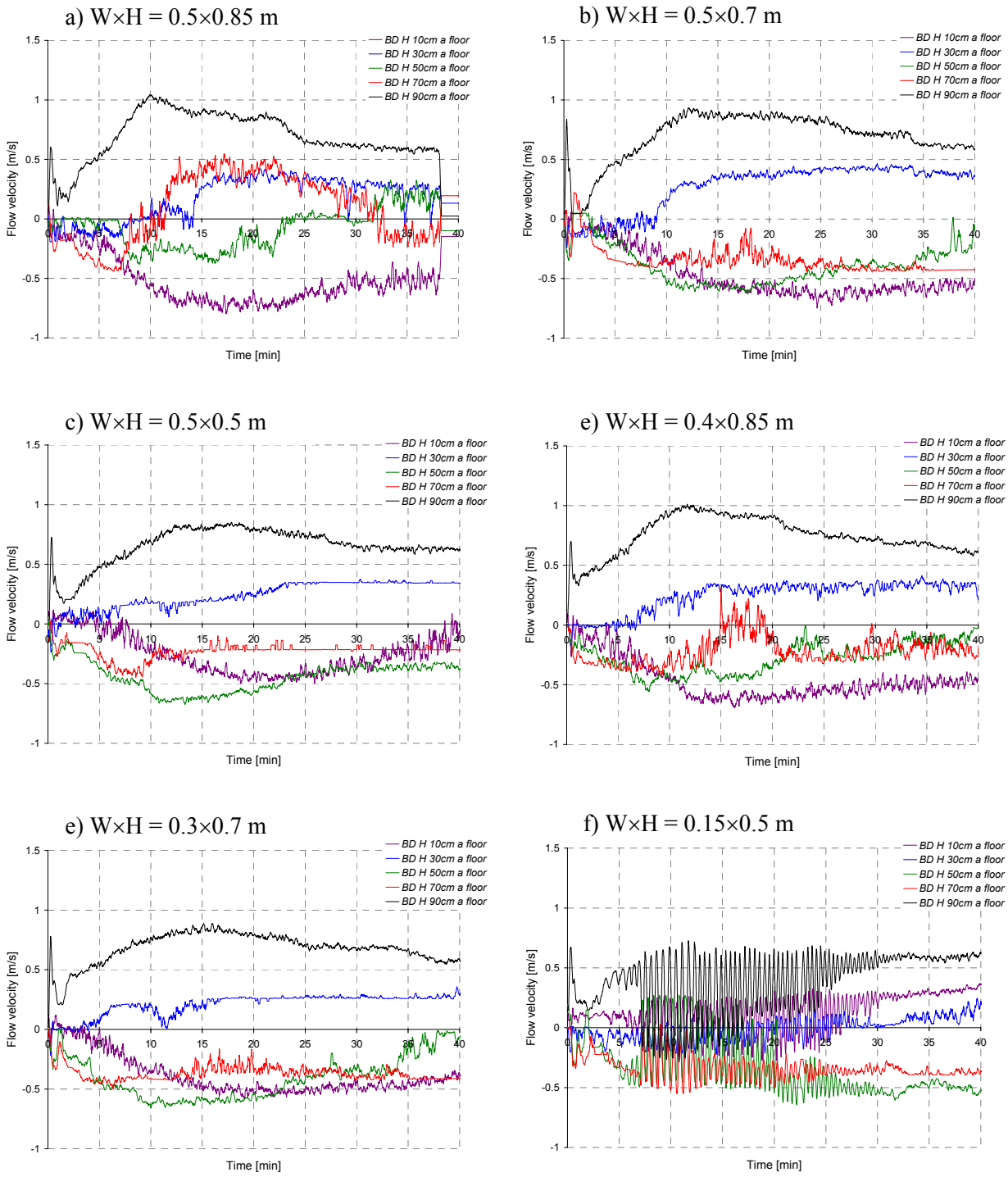

Figure 11. Velocity profiles at the centre of position H.

Figure 12 shows the incident radiative heat flux to the water-cooled Gunners meters positioned at the centre of the floor, the ceiling and the wall at K+ in Figure 2. Following the build up of a hot gas layer, effectively shielding the ceiling and the wall and at the same time adding to the thermal insult of the floor, the radiation heat flux towards the floor reach a level that would cause auto-ignition of most (combustible) construction materials.

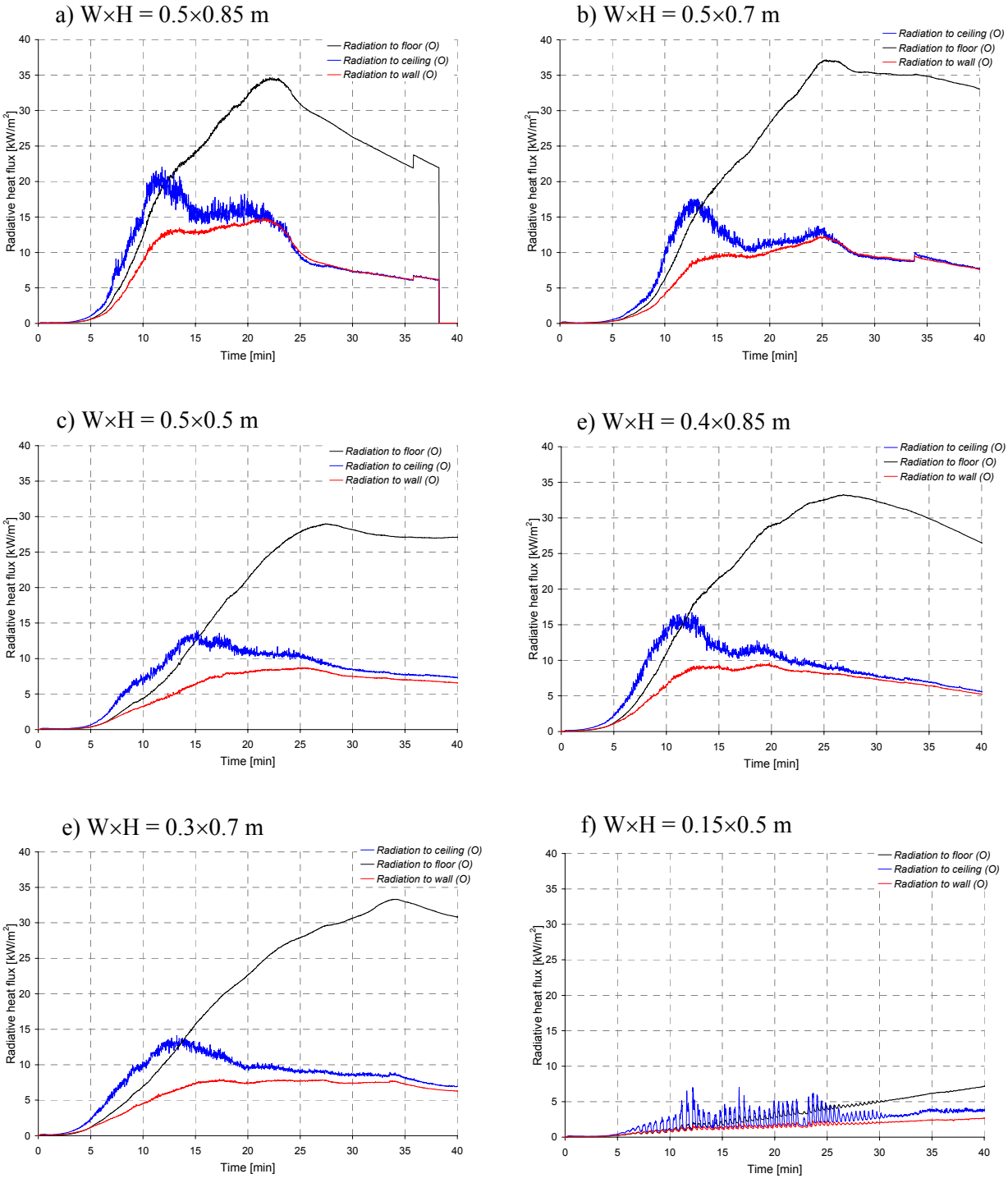

Figure 12. Thermal radiation to the centre of the floor, side wall and ceiling at position K+ as measured to a cold, water cooled, surface.

The fractions of the total heat flux that are due to thermal radiation at the wall and the ceiling are shown in Figure 13. Clearly, radiation plays an important role in this scenario, representing about 70% of the heat exposure to the side wall. Similarly, more or less half of the total heat flux to the ceiling is due to radiation.

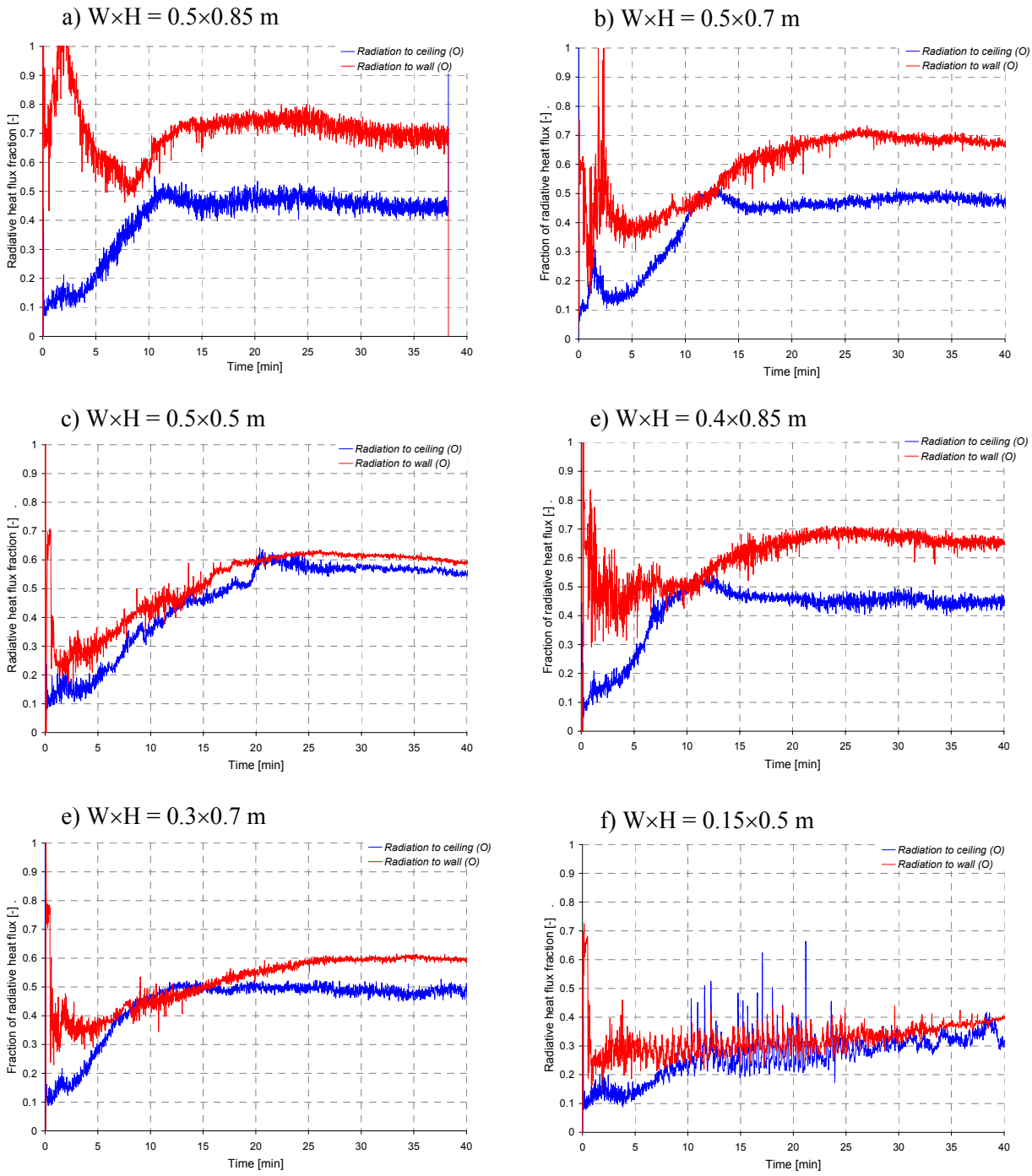

Figure 13. Fraction of the total heat flux that is due to thermal radiation.

The oxygen concentration within the enclosure, at 0.1 metres below the ceiling in the centre of position D is illustrated in Figure 14. For the general comparison these graphs also include the measured rate of heat release. Due to the fire becoming under-ventilated there is no complete correlation between the oxygen concentration in the room and the ventilation factor. This is particularly evident if one compares the rather well ventilated scenarios with the scenario having the smallest opening. It is interesting to note that apparently not all of the incoming oxygen is consumed in the fire but rather the concentration measurements at location D indicate the outflowing gaslayer to contain 2.5 vol% to 7.5 vol% of oxygen. This

may be attributed to the entrainment of fresh air from the inflowing air stream to the outflowing combustion gases.

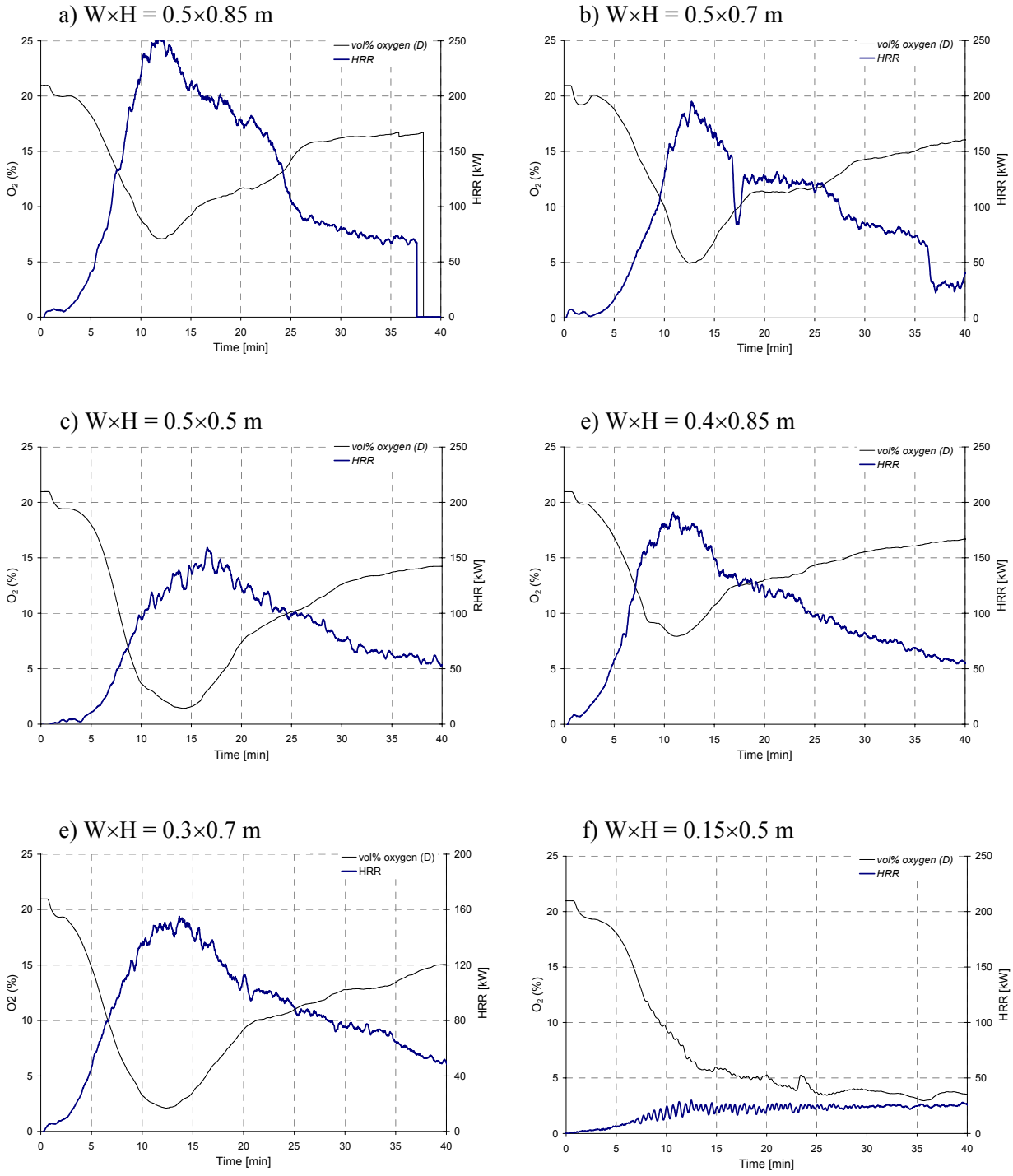

Figure 14. Oxygen concentration at position D as compared with the total heat release rate.

5. Sample calculations

Fire modelling using CFD (Computational Fluid Dynamics) techniques is a recognised field of research and of late it has, in essence, become part of the everyday work in fire safety design, the most frequently modelled phenomena being the smoke movement in buildings. In comparing simulations with experimental results, several independent expert users have shown that the CFD codes having fire specific models implemented (such as CFX, FDS and SOFIE for example) do well in this regard. Caution is however required since there are indeed fairly simple scenarios in which the models seem to fail in their prediction, one such example being a single space with high ceiling[25,26].

An important insight is that a CFD solution does not claim to provide the correct answer to every scenario. We are still referred to the use of rather incomplete models in describing the course of events following a fire. The problems have been highlighted from a number of "blind simulations" in which a number of expert users simulate a scenario without prior knowledge of the end-results. Not surprisingly, the simulation results have been found to be both user and code dependent. Similar exercises have been performed within the fire modelling community covering zone models as well as various CFD software[27,28].

The simulations presented in this report are all so-called "a-priori simulations" or blind simulations performed before the actual tests were carried out. The calculations were made using the program FDS[29]. The physics of under-ventilated fires are not fully understood and since the tests are more or less heavily under-ventilated there is little to suggest that the simulations will be successful given the rather crude models implemented into FDS.

5.1 The CFD model FDS

Most of the computer programs dealing with turbulent reacting flows are based on a set of numerical techniques referred to as the finite volume method (FVM), using the integral form of the conservation equations as starting point. The core equation of any such program is exemplified, for an arbitrary variable ϕ, in the equation below. From the left we have the time rate of change inside an arbitrary volume denoted Ω, then transport due to convection through the surfaces enclosing the volume and likewise, diffusion through the faces of the volume, the last term is a source referring to the destruction or production of ϕ within Ω[30].

$$\frac{\partial}{\partial t}\int_{\Omega}(\rho\phi)d\Omega + \int_{S}(\rho U)\phi\cdot \mathrm{n}dS = \int_{S}(\Gamma\nabla\phi)\cdot \mathrm{n}dS + \int_{\Omega} q_{\phi}d\Omega$$

In order to model the continuous phenomena of fluid flow, the physical space is subdivided into a large number of finite volumes, called control volumes, on which the governing

equations are discretised and solved using various finite difference approximations. Algebraic interpolation is used to determine variables on the faces of the control volumes, a potential source of error. Due to the limitations in computer power, the discretisation cannot be made sufficiently fine to include all the relevant physics. Turbulence, combustion, radiation and boundary layer effects are all examples of phenomena that require some kind of simplification and modelling.

In the boundary layer near the walls the turbulent flow is influenced by viscosity and is slowed down due to wall friction. This induces steep gradients in terms of turbulent viscosity and velocity, since the instantaneous velocity components are zero at the solid boundaries (no-slip boundary). Temperature and enthalpy gradients are also generated due to the difference between the solid- and gas-phase temperatures. To capture these gradients in a numerical simulation, the transport equations would need to be integrated through the entire wall boundary layer. Very small control volumes are required for this task, so small that the cost in computational time is too great for all but the most trivial scenarios. A common solution is to use some kind of semi-empirical wall function to model the characteristics of the boundary layer, perhaps the most well-known being the "law of the wall" approach[31].

In contrast, the CFD code FDS uses empirical correlations for the wall flow. Convective heat transfer to the wall, for example, is calculated using the largest value for the free and the forced convection respectively[29]

$$\dot{q}''_{convective} = \Delta T * \max\left[C\left|\Delta T\right|^{1/3}, 0.037 \frac{k\,\mathrm{Pr}^{1/3}}{L^{0.2}} \left(\frac{|\mathbf{u}|}{\nu} \right)^{0.8} \right]$$

FDS uses a rather simple method based on oxygen consumption calorimetry for estimating the local rate of heat release. The oxygen consumption is calculated from the mixture fraction and the corresponding rate of heat release can then be evaluated from:

$$\dot{q}''' = \dot{m}'''_{O_2} \Delta H_{c,O_2}$$

In addition, a scheme is employed for relating flame extinction to the temperature and the oxygen concentration. In principle, this appears to be useful in simulating under-ventilated fires, where most CFD codes fail to predict burning behaviour accurately*.

Another main challenge in fire modelling is heat transfer through thermal radiation which is of great importance in almost all fires of practical interest, representing a major contribution to the total heat flux. From a modelling standpoint, radiative heat transfer exerts its numerical

* Although this method will not make FDS capable of actually handling under-ventilated fires, it is likely that also this crude model makes the code perform better than it would have otherwise.

influence through the energy conservation equation, where it appears as a source term that needs to be modelled.

The radiation transfer equation ignoring scattering effects by soot, effectively assuming that all soot particles are small compared with the thermal radiation wavelength, is written

$$\frac{dI}{ds} = \kappa_a (I_b - I)$$

While soot has a rather simple spectral dependency the local soot concentration in and near the flame is not generally known. Moreover, since radiation is proportional to the temperature raised to fourth power, a seemingly small error in the prediction of the gas temperature, which is quite likely in FDS (as well as most CFD codes used by the fire modelling community) due to the simple combustion model, can have an unacceptable influence on the end-result. Thus, in order to minimize these effects in FDS, blackbody intensity, I_b, takes its traditional value only outside the flame zone. Inside the flame the thermal radiation is simply assigned as a fraction of the local heat release rate[31]. This simplification is likely to have a fundamental influence on the radiation heat flux prediction.

$$\kappa_a I_b = \begin{cases} \kappa_a \sigma T^4 / \pi & \text{outside flame} \\ \chi_{loc} \dot{q}''' / 4\pi & \text{inside flame} \end{cases}$$

FDS does, to some extent, sacrifice detail and accuracy to the benefit of easy of use and comutational speed. Moreover, the solver and boundary conditions are extremely stable.

5.2 Simulations

It must be kept in mind that the simulations that are presented in this section are a-priori simulations, performed in advance of the actual testing. The fire input was taken to be equvivalent to the heat release from unconfined burning of the wooden crib, see Figure 3.

Calculations were carried out for two different ventilation openings; the one with an opening width×height of 0.5×0.7 metres and the other with a width×height of 0.5×0.5 metres.

5.2.1 Simulation results including the 0.5×0.7 meter opening

A number of simulations were performed for the scenario with the 0.5×0.7 meter (width×height) opening, varying different parameters. The simulations presented here deals mainly with the influence of the computational mesh. Table 2 summarises the differences between the simulations.

Table 2. Summary of simulations, opening 0.5×0.7 metres

Simulation 1	Computational mesh: dx = dy = dz = 0.05 metres Computational domain is extended in front and above the corridor.
Simulation 1b	Computational mesh: dx = dy = dz = 0.05 metres Atmosphere boundary condition in the ventilation opening.
Simulation 2	Computational mesh: dx = dy = dz = 0.10 metres Computational domain is extended in front and above the corridor.
Simulation 2b	Computational mesh: dx = dy = dz = 0.10 metres Atmosphere boundary condition in the ventilation opening.
Simulation 4b	Computational mesh: dx = dy = dz = 0.02 metres Atmosphere boundary condition in the ventilation opening.

Figure 15 shows the measured heat release rate compared with the computational results. The simulations demonstrate a noticeable node dependency. Rather surprisingly, the simulations using the largest control volumes provide the better results.

In the simulations using an extended computational domain, in which the atmospheric boundaries have been applied away from the test rig, the combustion zone moves towards the opening after the oxygen has been depleted within the compartment. This exterior burning is the reason to why there is a second peak in these cases. Clearly, there is room for model improvement in this area.

The calculated maximum heat release rate from the enclosure fire shows a correlation with the characteristic fire diameter, defined as

$$D^* = \left(\frac{\dot{Q}}{\rho_\infty c_p T_\infty \sqrt{g}} \right)^{2/5}$$

The maximum calculated $\dot{Q}$ consistently corresponds to a D^* of approximately 10 times the side lenght of the control volumes in all the simulations, that is $D^* / \delta x \approx 0.1$. If there is a physical reason to this has not been analysed, it may be a feature of FDS.

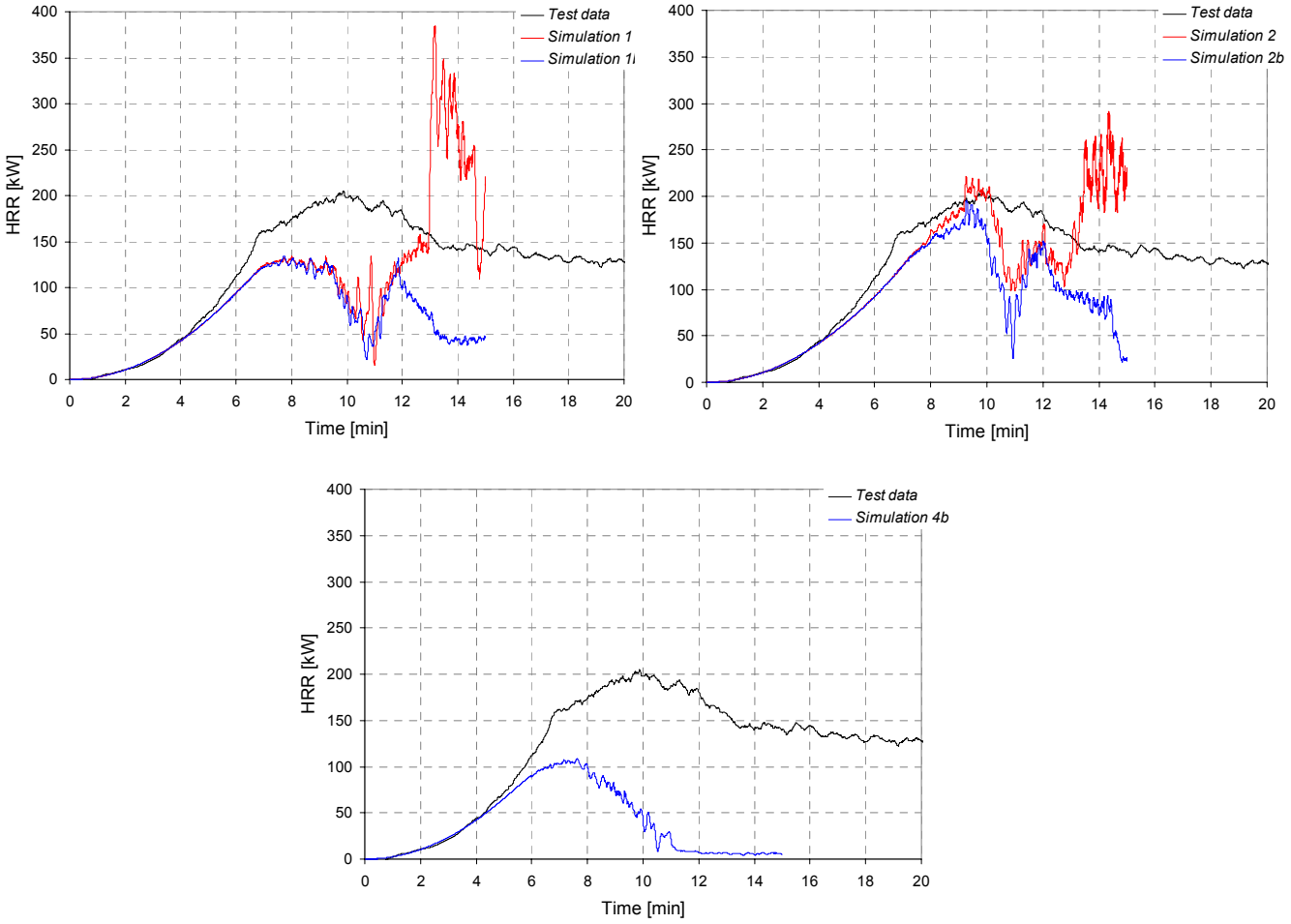

Figure 15. Measured heat release rate compared with computational results.

The concentration of oxygen by volume was measured and calculated at position D 0.9 metres above the floor, see Figure 2. A comparison of the test data with the calculations is shown in Figure 16. The size of the computational domain and the location of the atmospheric boundaries seem to be of no importance however, there is a noticeable node dependency.

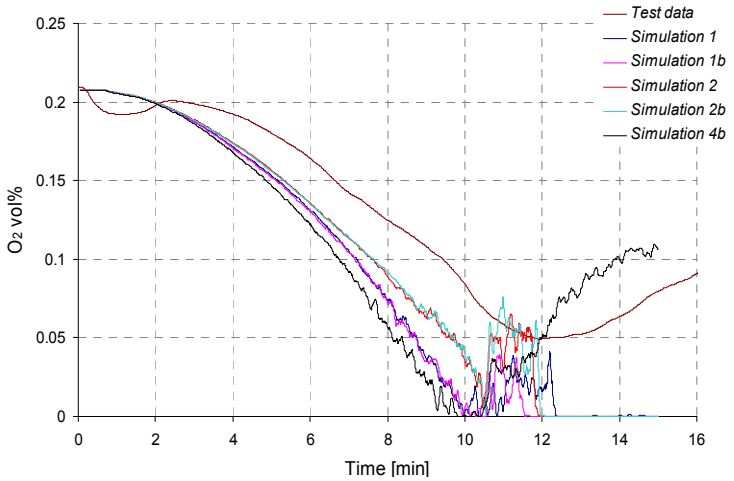

Figure 16. Oxygen concentration (vol %) within the enclosure.

The gas temperature in a vertical centreline at position H, as defined by Figure 2, is consistently underestimated by the simulations. In Figure 17 the temperature measurements are compared with computations at a single point, 0.10 metres below the ceiling, also a comparison is made for the temperature distribution in the vertical centreline at a time 4 minutes after ignition, where the measured and calculated heat release rate are still the same.

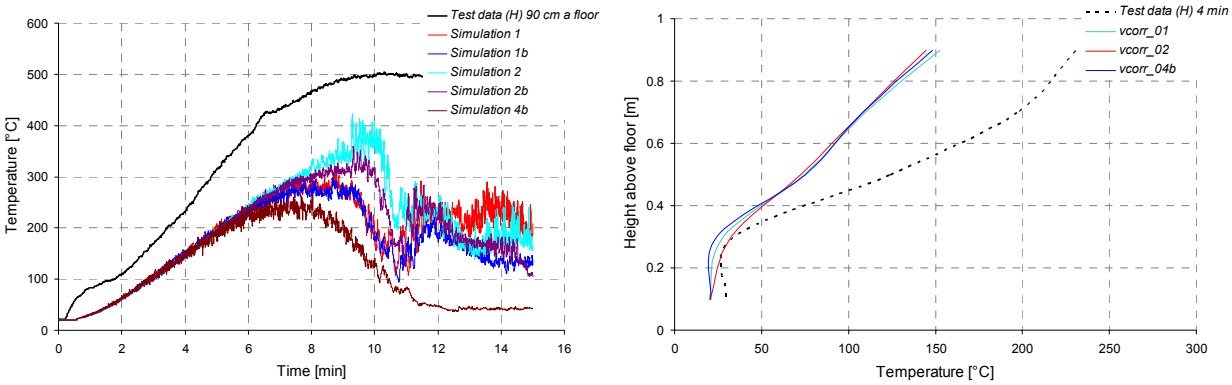

Figure 17. Gas temperatures at position H, vertical centreline. a) 0.1 metres below the ceiling and b) distribution at time 4 minutes after ignition.

While the gas temperature at H is consistently under-estimated by the calculation, the temperature in the ventilation opening is to the most part over-predicted, see Figure 18. Thus, the heat loss to the inner structure seems to be under-estimated in the front part of the enclosure but over-estimated at the inner parts.

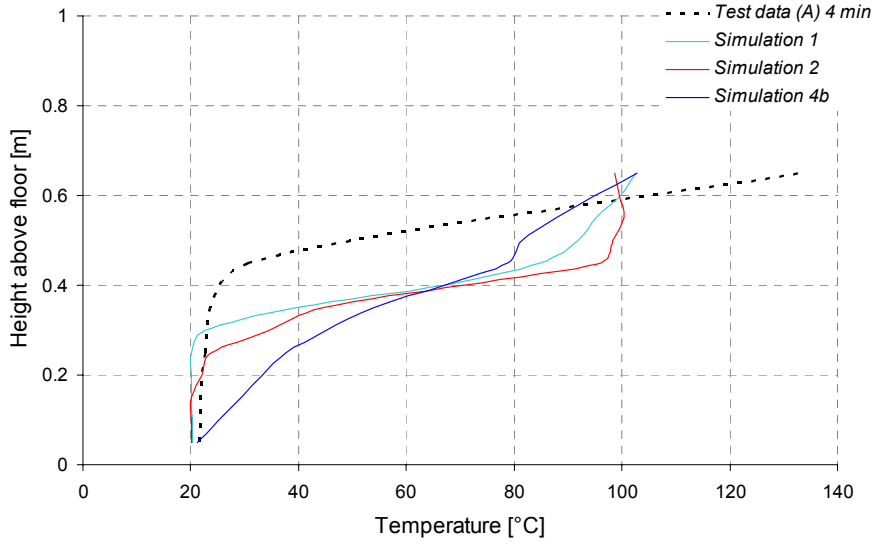

Figure 18. Comparison between measured and calculated gas temperature in the centre of the vent.

In Figure 19 the flow field is shown at two different points in time, 6 minutes and 8 minutes after ignition respectively. The pictures are consistent with the observation during the tests showing different layers of smoke, although not as pronounced as in the test data, Figure 11.

a)

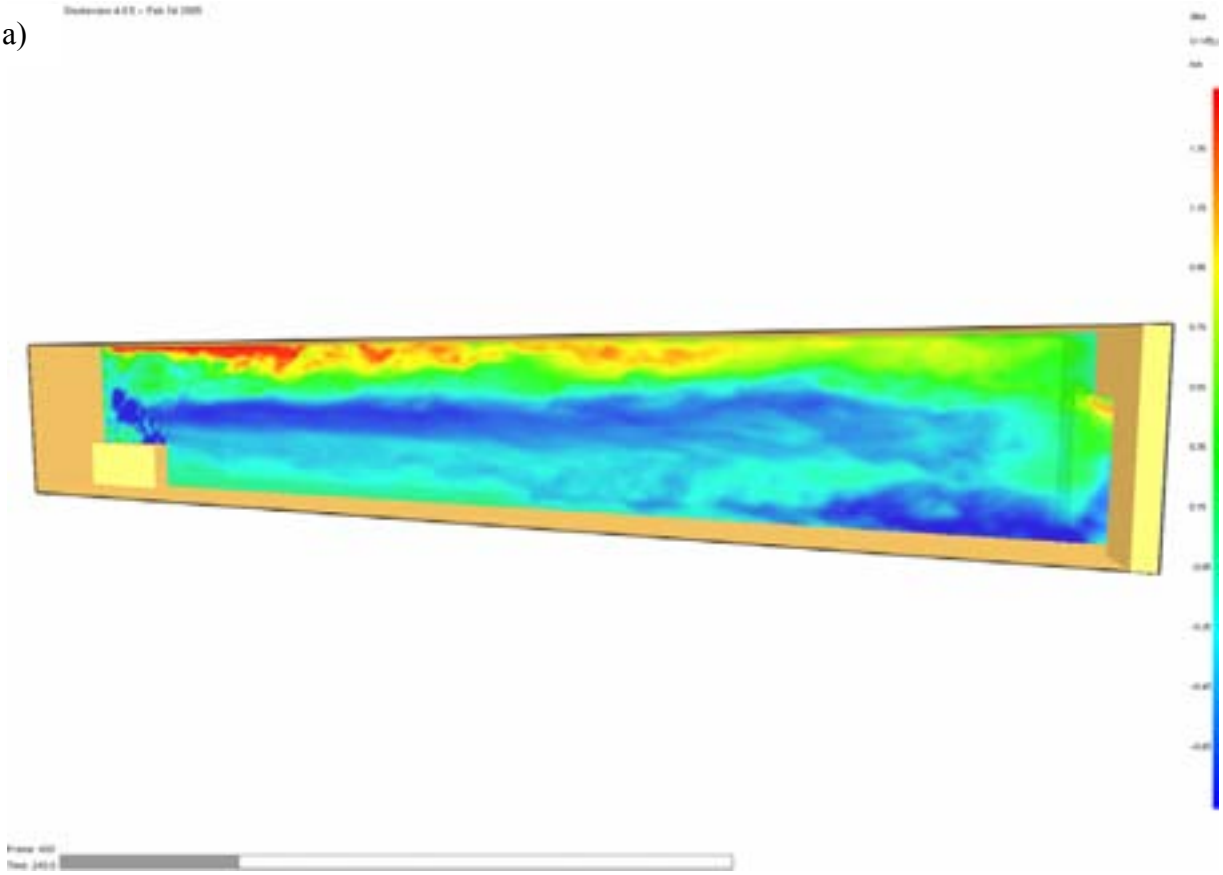

b)

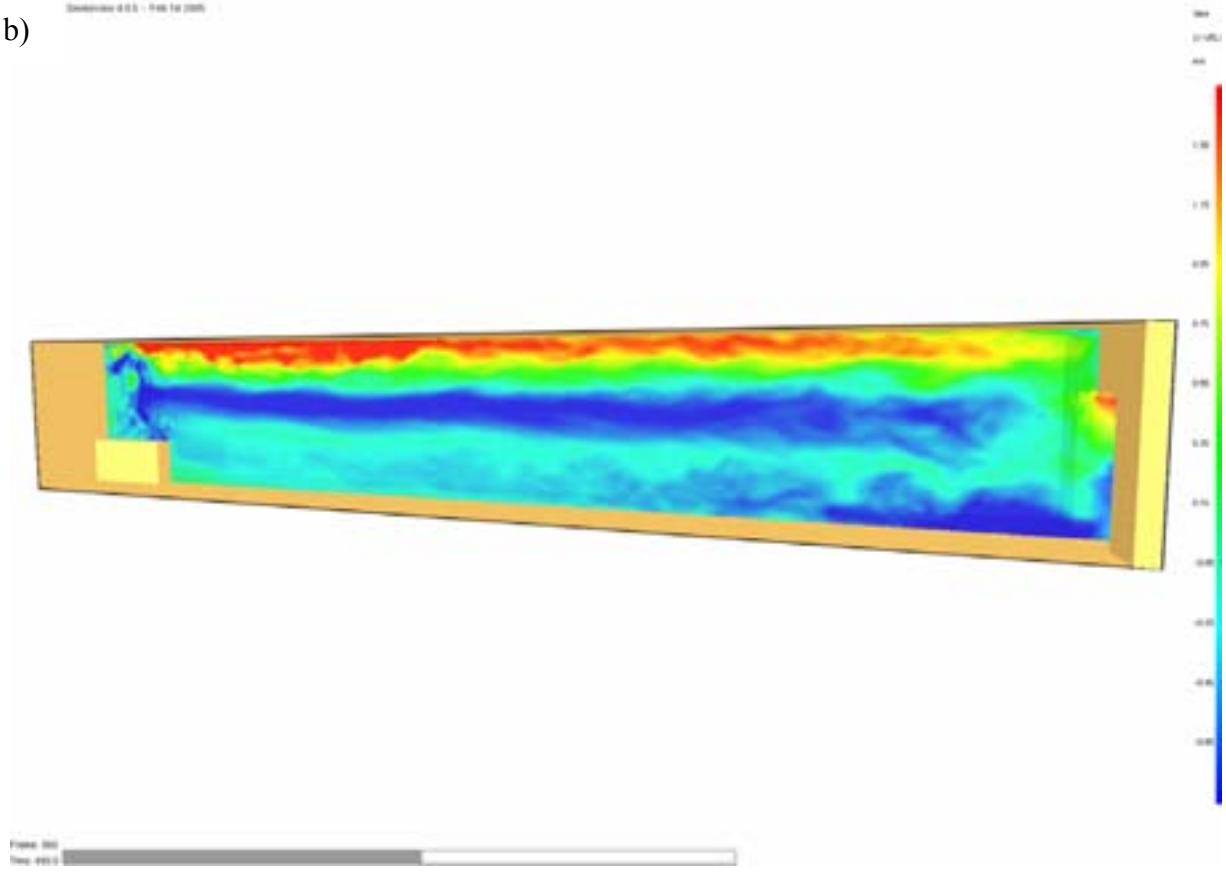

Figure 19. Instantaneous snap-shots of the flow field at a) 4 minutes after ignition and b) 8 minutes after ignition.

5.2.2 Simulation results including the 0.5×0.5 meter opening

An analogous set of simulations were carried out with the ventilation opening reduced to 0.5×0.5 metres. The identifiers of the simulations that are presented in this report and the difference between them are summarised in Table 3.

Table 3. Summary of simulations, opening 0.5×0.5 metres.

Simulation 5	Computational mesh: dx = dy = dz = 0.025 metres Computational domain is extended in front and above the corridor.
Simulation 6b	Computational mesh: dx = dy = dz = 0.02 metres Atmosphere boundary condition in the ventilation opening.
Simulation 7b	Computational mesh: dx = dy = dz = 0.05 metres Atmosphere boundary condition in the ventilation opening.
Simulation 8b	Computational mesh: dx = dy = dz = 0.10 metres Atmosphere boundary condition in the ventilation opening.

Again, it should be pointed out that the simulations are blind simulations performed in advance of the experiments. Furthermore, in this scenario, because of the efficient containment of the combustion gases that follows from the lowering of the soffit, there seem to be a substantial time delay in the oxygen calorimetery measurements. The measured heat release based on the oxygen consumption method was therefore corrected in time using the data from the measurement if the fuel mass loss. This could have been done also in the previous scenario however, the effect was not as prounounced in this case and no correction was made.

The measurement data on the rate of heat release are compared with the computational results in Figure 20. There is little difference between the simulations concerning the general behaviour of the burning rate although, basically, the larger the control volume the higher the peak heat release rate becomes before decreasing.

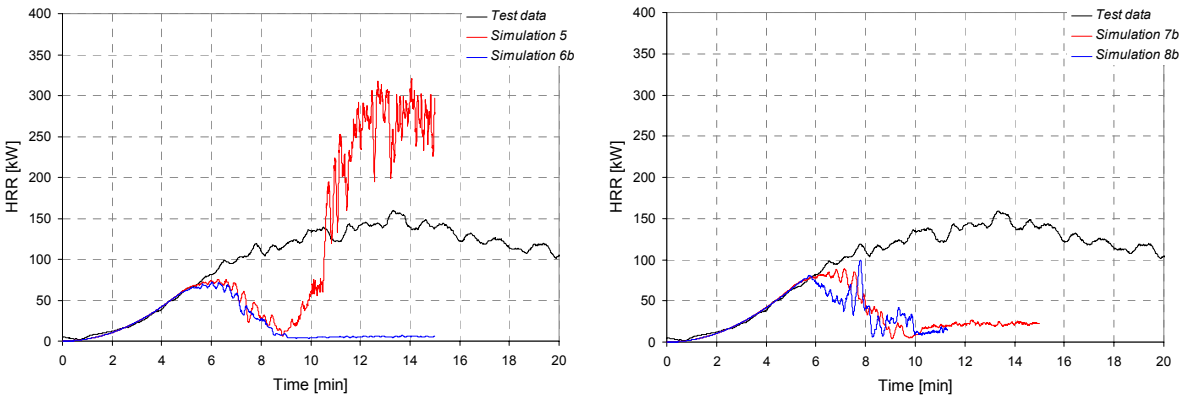

Figure 20. Calculated heat release rate compared with measurements.

As the concentration of oxygen in the corridor becomes close to zero the heat release rate decreases ending up at only a hint of burning within the enclosure when a zero oxygen concentration is reached. At this time, although highly non-physical, the model suggests the combustion zone to be fixed at the ventilation opening. In the simulation in which the computational domain has been extended outside the enclosure, the burning continues with the major external flaming attached to the vent. FDS includes routines that require a sufficient amount of oxygen and heat in order for burning to be sustained. This, however, does not hold back the propagation of the combustion zone across the length of the corridor which sustains itself with heat and moves towards the vent as it consumes the available oxygen.

In the simulations having the computational boundary in the opening, no external burning is possible and only a very small fire continues to burn in the opening even as the oxygen concentration within the enclosure subsequently increases. This behaviour is exemplified in Figure 21 in which both experimental and calculated results are shown.

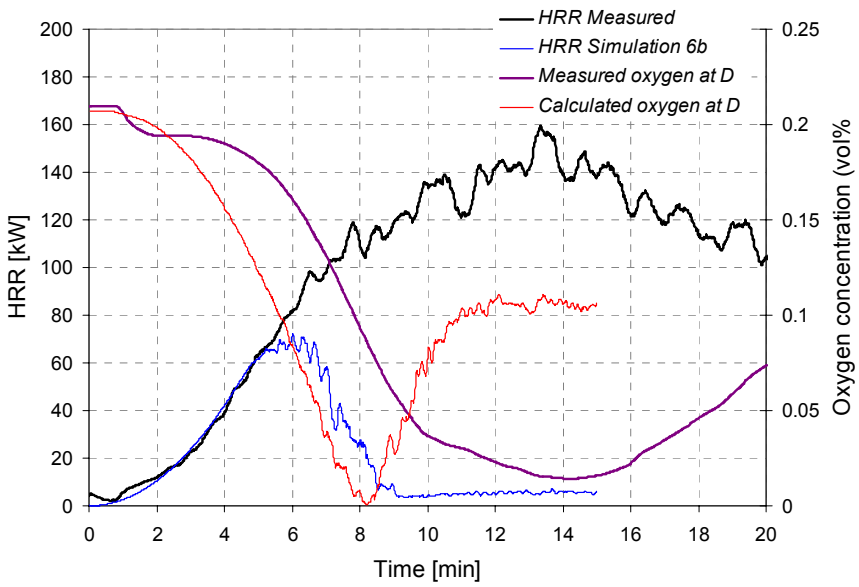

Figure 21. Measured oxygen concentration and HRR compared with computational results from the calculation tagged “Simulation 6b”.

In Figure 22 the predicted temperature distribution 4 minutes after ignition at position H and A (ventilation opening) is compared with the thermocouple measurements. Again, it is clear that the predicted heat loss does not completely match that of the test. The almost perfect prediction in the vertical centreline of H is not matched by the results in the ventilation opening.

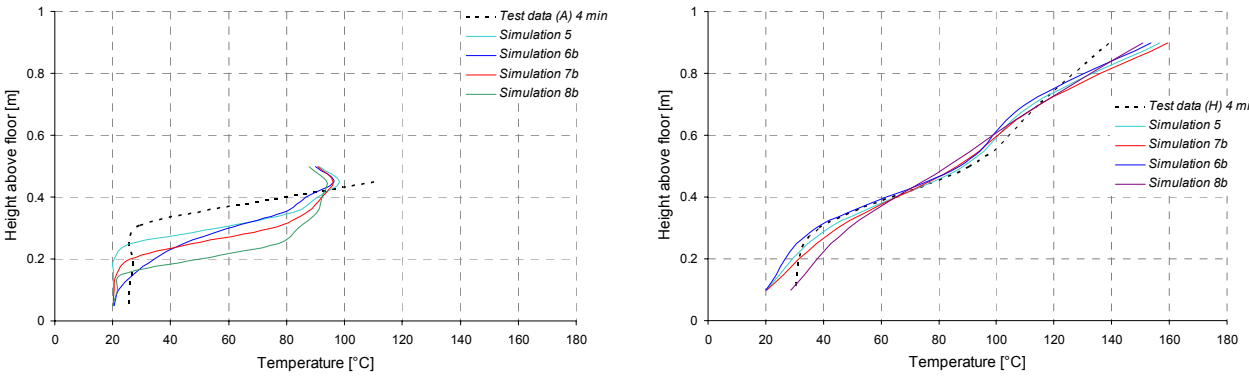

Figure 22. Comparison of the measured temperatures and the predictions at positions A and H, 4 minutes after ignition.

In Figure 23 the flow velocity predictions obtained from Simulation 5 are compared with measurements from position H at 0.5 metres and 0.9 metres above the floor respectivelty. The results are reasonable considering the extremely low velocities, being close to the measuring capabilities of the pressure transducers.

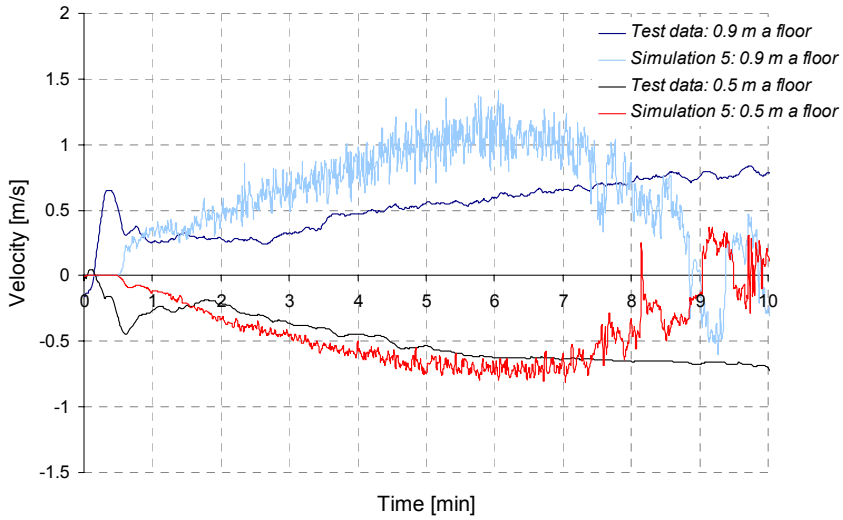

Figure 23. Measured velocity during the first 10 minutes of the test compared with computational results.

6. Summary and conclusions

An experimental study consisting of 14 tests has been carried out in a corridor-like enclosure. With the exception of tunnel fire research that has just recently become a popular field of research, very few fire investigations can be found concerning long and narrow rooms. The test rig that was used in this work has been of an intermediate scale but it may be difficult to scale it properly partly due to the major influence of thermal radiation compared with the convective flow, the thermal radiation flux representing between 50 % and 70 % of the total heat flux to the ceiling and the walls near the fire.

Based on the heat balance in the opening and the measured peak heat release rate a good correlation could be derived linking the ventilation factor to the maximum heat release rate. Such a correlation can be readily used to obtain an estimate of the maximum burning rate within a corridor or a tunnel. Measurements of the oxygen concentration within the enclosure indicate that although the supply of air from the ventilation opening puts a constraint on the maximum heat release not all oxygen is consumed by the fire.

A-priori simulations (performed in advance of the actual testing) using the CFD program FDS show good or reasonable agreement with the experimental data during the developing phase but diverges in the later stages when the fire is turning ventilation controlled. The discrepancy between measurements and the calculation seem, to a part, to be attributed to erroneously calculated heat losses through the solid boundaries of the enclosure.

It has thus been shown that the rate of burning in a long and narrow enclosure shows a nearly linear relationship with the ventilation factor, $A\sqrt{H}$. It has further been demonstrated that although providing fair results in well-ventilated fuel-controlled fires, advanced fire simulation programs lack in the predictive capabilities regarding ventilation-controlled scenarios. There is a clear need of improved, more flexible combustion models to address the critical part of fire development including a fire becoming ventilation-controlled and the onset of flashover.

References

1 Heskestad G., Hill J. P., Experimenal Fires in Multiroom/Corridor Enclosures, Factory Mutual Research Corporation, NBS-GCR-86-502, 1986.

2 Delichatsios M. A., Silcock G. W. H.., Liu X., Delichatsios M., Lee Y.-P., Mass pyrolysis rates and excess pyrolysate in fully developed enclosure fires, Fire Safety Journal vol 39 pp 1-21, 2004.

3 Carvel R. O., Jowitt P. W., Drysdale D. D., The Influence of Tunnel Geometry and Ventilation on the Heat Release Rate of a Fire, Fire Technology, 40, pp 5-26, 2004.

4 Ingasson H, Lönnermark A., Heat release rates from heavy goods vehicle trailer fires in tunnels, Fire Safety Journal, 2005.

5 Lönnermark A., Ingasson H., Gas temperatures in heavy gods vehicle fires in tunnels, Fire Safety Journal, vol 40, 2005.

6 Egan M. R., and Litton C. D., Wood crib fires in a ventilated tunnel, Bureau of Mines Report of Investigations 9045, United States Department of the Interior, 1986.

7 Ingasson H., Nireus K., Werling P., Fire Tests in a Blasted Rock Tunnel, FOA-R--97-00581-990--SE, Scientific report, November 1997.

8 Jones W. W., Quintiere J. G., Prediction of corridor smoke filling by zone models, Combustion Science and Technology, Vol 35, pp 239-253, 1984.

9 Nelson H. E., Deal S., CORRIDOR: A Routine for Estimating the Initial Wave Front Resulting from Heigh Temperature Fire Exposure to a Corridor, NISTIR 4869, NIST, Gaithersburg, July 1992.

10 Steckler K. D., Fire Induced Flows in Corridor - A Review of Efforts to model Key Features, NISTIR 89-4050, NIST, Gaithersburg, July 1989.

11 Jones W. W., Takayuki M., Baum H. R., Smoke Movement in Corridors - Adding the Horisontal Momentum Equation to a Zone Model, Proceedings of 12th Joint Panel Meeting of the UJNR Panel on Fire Research and Safety, 1992.

12 Forney G. P., A Note on Improving Corridor Flow Predictions in a Zone Fire Model, NISTIR 6046, NIST, Gaithersburg, 1997.

13 Satoh K., Miyazaki S., A Numerical Study of Large Fires in Tunnels, Report of Fire Research Institute if Japan, No. 68, pp 19-34, 1989.

14 Tuovinen H., Simulation of Combustion and Fire-Induced Flows in Enclosures, PhD Thesis, Lund University, Lund, 1995.

15 McCaffrey B. J., Quintiere J. G., Harkleroad M. F., Estimating Room Fire Temperatures and the Likelihood of Flashover Using Fire Test Data Correlations, Fire Technology, Vol 17, No 2, pp 98-119, 1981.

16 Babrauskas V., Estimating Room Flashover Potential, Fire Technology, vol 16, pp 94-103, 1980.

17 Janssens M., Parker W. J., Oxygen Consumption Calorimetry, Heat Release in Fires, Ch 3, Ed. Babrauskas V., Grayson S. J., Elsevier Applied Science, 1992.

18 Saito, Fire Safety Journal pp139-182, 1992.

19 McCaffrey B, Flame Heights, The SFPE Handbook of Fire Protection Engineering, Chapter 2-1, 2nd Ed., 1995.

20 Quintiere J., McCaffrey B. J., Kashiwagi T., A Scaling Study of a Corridor Subject to a Room Fire, Combustion Science and Technology, Vol. 18, pp1-19, 1978.

21 Williams F. A., Scaling Mass Fires, Fire Research Abstracts and Review, pp 1-23, 1969.

22 de Ris J., Kanury A. M., Yuen M. C., Pressure Modeling of Fires, 15th Symposium (Int) on Combustion, The Combustion Institute, pp 1033-1044, 1973.

23 Walmerdahl P., Werling P., Fire Growth and Spread - An experimental study in model-scale, FOI-R--0907--SE, 2003.

24 Carlsson J., Werling P., Vassfjord J., Eriksson M., Mätdata - Underventilerad brand i corridor 2005, FOI MEMO 1530, 2005.

25 Andersson P., Blomqvist J., Smoke Detection in Buildings with High Ceilings, Brandforsk project No 628-011, SP-report 2003-33, Borås, 2003.

26 William D. D., Notarianni K A., McGrattan K. B., Comparison of Fire Model Predictions with Experiments Conducted in a Hangar with 15 meter Ceiling, NISTIR 5927, BFRL, NIST, Gaithersburg 1996.

27 Hostikka S., Keski-Rahkonen O., Results of CIB W14 Round Robin for Code Assessment Scenario B. Draft 31/08/98, VTT Technical Research Centre of Finland, 1998.

28 Grandison A.J,.Galea E.R., Patel M.K., Fire modelling standards/benchmark - Report on Phase 1 Simulations, Fire Safety Engineering Group, University of Greenwich, London, 2001.

29 .McGrattan K. B. ed.,Fire Dynamics Simulator (Version 4) – Technical Reference Guide, National Institute of Standards and Technology, NISTIR 6783, 2004.

30 Patankar S. V., Numerical Heat Transfer and Fluid Flow, Series in computational methods in mechanics and thermal science, Taylor & Francis, ISBN 0-89116-522-3, 1980

31 Wilcox, D. C., Turbulence Modelling in CFD, DCW Industries Inc, 2001.